IEEE Access
Multidisciplinary | Rapid Review | Open Access Journal

Received June 9, 2020, accepted June 13, 2020, date of publication June 22, 2020, date of current version July 2, 2020.

Digital Object Identifier 10.1109/ACCESS.2020.3004241

Extended Disturbance Observer-Based Integral Sliding Mode Control for Nonlinear System via T–S Fuzzy Model

SOUNGHWAN HWANG[1] **AND HAN SOL KIM**[2]
[1]Department of Electrical and Electronic Engineering, Yonsei University, Seoul 120-749, South Korea
[2]Department of Control and Automation Engineering, National Korea Maritime and Ocean University, Busan 49112, South Korea

Corresponding author: Han Sol Kim (hansol@kmou.ac.kr)

This work was supported by the National Research Foundation of Korea (NRF) grant funded by the Korean Government (MSIT) under Grant NRF-2019R1G1A1099286.

ABSTRACT In this paper, an extended disturbance observer-based integral sliding-mode control for a nonlinear system is proposed by the Takagi-Sugeno (T–S) fuzzy model approach. The proposed method focuses on two points: First, improving the design flexibility of integral fuzzy sliding-mode control (IFSMC) by transforming a conventional T–S fuzzy model structure into a novel form. Second, expanding a previous disturbance observer-based control (DOBC) concept by introducing a Fourier analysis to deal with the non-periodic form of disturbance. By using the modified form of the fuzzy model, a novel sliding surface combined with estimated disturbance through several fuzzy disturbance observers (FDOB) is suggested. Besides, a sufficient condition for guaranteeing asymptotic stability of the sliding dynamic with H_∞ control performance is proposed by applying a proper Lyapunov function with the linear matrix inequality (LMI) concept. Furthermore, a reachability problem of the proposed sliding surface is also handled by introducing another Lyapunov function. Finally, the effectiveness of the proposed method is demonstrated by comparing previous studies, which focused on robust control techniques, based on the simulation results of an inverted-pendulum system.

INDEX TERMS Takagi-Sugeno (T–S) fuzzy model, robust control, sliding-mode control (SMC), disturbance observed-based control (DOBC), fuzzy disturbance observer (FDOB), linear matrix inequality (LMI), Lyapunov stability analysis, Fourier analysis.

I. INTRODUCTION

Over the last few decades, as systems become more complex and sophisticated, many nonlinear system control techniques, such as sliding-mode control (SMC), adaptive control, and model predictive control, have successfully introduced and suggested [1]–[6], [32]–[43]. Among them, one powerful method is the Takagi–Sugeno (T–S) fuzzy model approach [5], [6]. The key idea of the T–S fuzzy modelling technique is that it allows us to represent a nonlinear system as a linear combination of state space models and its corresponding membership functions, which indicates that it is possible to apply linear control theories [1], [2] to the T–S fuzzy model. Due to its powerful advantages, various studies, including fuzzy filter [7], [8], [39], fuzzy tracking control [9], [41], observer-based control [10], and sampled-data approach [11], have been successfully developed and well established. Besides foregoing studies, robust control techniques based on the T–S fuzzy model [6], [12]–[17], [34], [39], [44] also have been greatly studied since guaranteeing a certain stability of the system is a crucial issue in designing a controller. In particular, those techniques have focused on how to enhance robustness through a designed controller by analyzing various disturbance factors, such as plant uncertainty, matched disturbance (i.e. the disturbance acting on the control input channel), and mismatched disturbance (i.e. disturbance not acting on the control input channel). For example, in [12], a robust stabilization toward the plant uncertainty was successfully derived, and in [44], the second-order SMC technique [36]–[38] was proposed to alleviate the influence of chattering phenomenon.

The associate editor coordinating the review of this manuscript and approving it for publication was Shihong Ding.

Among aforementioned robust control techniques, an integral fuzzy sliding-mode control (IFSMC) [13]–[15], and fuzzy disturbance observer-based control (FDOBC) [16], [17] have received a great interest in that IFSMC eliminates a reaching phase, which was one of the phenomena of conventional SMC and successfully attenuates the influence of the matched disturbance, and FDOBC directly compensates the influence of mismatched disturbance generated from an exogenous system by using an estimated disturbance. Despite such great achievements, there are still some constraints to be improved and polished. The detailed limitations of previous studies and some improvements that need to be made will be illustrated in order.

As mentioned before, a matched disturbance is a norm bounded disturbance signal that acts on the control input channel [32], [33]. To deal with this problem, in [18], an integral sliding mode control (ISMC) was first introduced. Due to its robustness, the ISMC method combined with the T–S fuzzy model (i.e. IFSMC) has been successfully developed through many studies [13]–[15]. Although the achievements of the IFSMC approach have extensively proved, however, many previous studies have assumed that input matrices of the T–S fuzzy model have the same value regardless of its fuzzy rules. The reason why the structure of input matrices of the fuzzy model is important in designing the IFSMC is that input structure plays a key role in determining an equivalent control law when deriving a sliding dynamic [18, eq. (9)]. However, that assumption can be highly restrictive and cannot be widely applied to practical examples because systems which we are interested in maybe highly different due to its inherent characteristics. In [13], this problem was partly solved due to a characteristic of the plant, not depending on a general theoretical approach. Moreover, that problem was also handled in [14], [15], however, the proposed methods are still hard to implement. To sum up, establishing a general framework of the IFSMC regardless of the structure of input matrices can be regarded as a great motivation.

Furthermore, taking into account a mismatched disturbance when designing a controller is another important issue as considering the matched disturbance. Given this point, in [19], a first disturbance observer-based control (DOBC) approach was introduced based on the frequency domain, and it received great attention in that directly compensating the mismatched disturbance generated from an exogenous system, via disturbance observer (DOB). As the focus of DOBC theme shifts from the frequency domain to the time domain, many DOBC and FDOBC studies based on the state-space framework have been successfully developed [16], [17], [20]–[23], [30]. Although previous studies have proved their effectiveness, however, those studies assumed that the form of the mismatched disturbance is defined as a neutral stable sinusoidal function with a certain period and frequency or a decaying exponential function as time flows. In many practical cases, the form of disturbance may vary from case to case, which means that it may follow a periodic or non-periodic sinusoidal signal. All things considered, developing a general framework of designing the FDOBC method even if the mismatched disturbance is a non-periodic neutral stable (NPNS) signal can be considered as a great catalyst in terms of proposing a robust control technique.

Motivated by the aforementioned statements, this paper proposes a novel theoretical framework combined with IFSMC and FDOBC concepts to deal with the matched disturbance and mismatched disturbance simultaneously. The main contributions of this paper are listed as follows:

1) First, to clear up the problem as mentioned in the third paragraph, the T–S fuzzy model is transformed into a new structure to successfully derive a sliding dynamic. The transformed one is a suitable form when designing an IFSMC, thus, the proposed method provides a general theoretical approach when designing an IFSMC and enhances the design flexibility when dealing with various types of systems having different input matrices.
2) Second, to deal with an NPNS mismatched disturbance signal properly, Fourier analysis is applied to that signal to filter out dominant periodic signals (DPS) before formulating the FDOBC. By filtering out several DPS signals within a given time interval, the NPNS signal can be handled by several distinct FDOBs, which indicates that it is a worthwhile perspective in that the previous DOBC concept can be enlarged into the NPNS types of signals.
3) Third, to stabilize the augmented system merged with a sliding dynamic, and several fuzzy disturbance observers (FDOB), a sufficient linear matrix inequality (LMI)-based condition with H_∞ performance is presented using a proper Lyapunov function. Moreover, a reachability problem subject to the proposed sliding surface is also successfully handled by using another Lyapunov function properly.
4) Last, the effectiveness of the proposed method is verified by the simulation results of the inverted pendulum system. The proposed method shows a better performance compared to the previous studies [6, Th.14], [13], [17], which proposed robust control techniques by covering many diverse disturbances.

The present work is outlined as follows: In Section II, modifying T–S fuzzy model into a suitable form for ISFMC and designing FDOBs and ISFMC subject to an NPNS disturbance via Fourier analysis are presented. In Section III, the main results of this paper are proposed. In Section IV, the simulation results of the inverted pendulum system are provided and the effectiveness of the proposed method is demonstrated. In Section V, conclusion and future work are given. Finally, some supplements for Section II and detailed proof of Theorem 1 are presented in the Appendix section to the efficient placement of the paper.

Notations: The symbol $He\{A\}$ denotes $A + A^T$, A^+ indicates the left pseudo inverse of A, $\mathcal{R}^{n\times n}$ indicates all real matrices with order $n \times n$, $\lambda_{\max}(A)$ is referred to as a maximum eigenvalue of A, $\lambda_{\min}(A)$ is referred to as a minimum

eigenvalue of A and * represents the symmetric term in a square matrix for notational simplicity.

II. PRELIMINARIES AND PROBLEM FORMULATION

A. T–S FUZZY MODEL

The T–S fuzzy model used in this work is described through the following IF-THEN rules [5], [6]:

$$\begin{aligned}&\text{Plant rule } i:\\&\text{IF } x_1(t) \text{ is } M_1^i \text{ and } x_2(t) \text{ is } M_2^i \cdots \text{ and } x_z(t) \text{ is } M_z^i,\\&\text{THEN } \begin{cases}\dot{x}(t) = A_i x(t) + B_i\left[u(t) + H(x(t))\right] + B_{di} d(t),\\ y(t) = C_i x(t),\end{cases}\end{aligned} \tag{1}$$

where $i \in \mathcal{I}_r = \{1, 2, \ldots, r\}$, r denotes the total number of the IF-THEN rules, $x_j(t)$ for $j \in \mathcal{I}_z$ is the premise variable, and M_j^i denotes the jth fuzzy set corresponding to the ith fuzzy rule. Furthermore, $x(t) \in \mathbb{R}^n$ denotes a state vector of the system, $u(t) \in \mathbb{R}^m$ indicates a control input, $y(t) \in \mathbb{R}^q$ denotes an output of the system, and $d(t) \in \mathbb{R}^1$ denotes a mismatched disturbance generated from an exogenous system following the form of an NPNS signal, satisfying an initial condition $d(0) = 0$ and it does not belong into the control input channel. Moreover, $H(x(t)) \in \mathbb{R}^m$ implies a matched disturbance acting on the control input channel. Additionally, the system matrices $A_i \in \mathbb{R}^{n\times n}$, $B_i \in \mathbb{R}^{n\times m}$, $B_{di} \in \mathbb{R}^{n\times 1}$, and $C_i \in \mathbb{R}^{q\times n}$ are known real matrices with appropriate dimensions.

Subsequently, by applying the singleton fuzzifier, product inference engine, and center-average defuzzification [5], [6] to the fuzzy IF-THEN rule (1), the T–S fuzzy model (1) can be inferred as follows:

$$\begin{aligned}\dot{x}(t) &= \sum_{i=1}^{r} w_i(x(t))\Big\{A_i x(t) + B_i\left[u(t) + H\left(x(t)\right)\right] + B_{di} d(t)\Big\},\\ y(t) &= \sum_{i=1}^{r} w_i(x(t)) C_i x(t),\end{aligned} \tag{2}$$

where detailed descriptions are given as follows:

$$\begin{aligned}&\sum_{i=1}^{r} w_i(x(t)) = 1, \quad w_i(x(t)) \in [0, 1],\\ &w_i(x(t)) = \frac{\mu_{M_1^i}(x_1(t)) \times \cdots \times \mu_{M_z^i}(x_z(t))}{\sum_{k=1}^{r}(\mu_{M_1^k}(x_1(t)) \times \cdots \times \mu_{M_z^k}(x_z(t)))}.\end{aligned} \tag{3}$$

where $w_i(x(t))$ denotes a normalized membership function consisting of $x_j(t)$ and $\mu_{M_j^i}(x_j(t))$ which denotes a membership function corresponding to the fuzzy set M_j^i.

In this paper, the following assumptions are needed for designing an IFSMC and FDOB.

Assumption 1 [16]: The matched disturbance $H(x(t))$ and mismatched NPNS disturbance $d(t)$ are norm bounded and satisfy the following inequality condition:

$$\|H(x(t))\| \le \epsilon \|x(t)\|, \quad \|d(t)\| \le \alpha, \tag{4}$$

where ϵ, α are appropriate positive constants.

Assumption 2: In this paper, unlike previous studies [16], [25], [26], it is assumed that the form of input matrix B_i with $i \in \mathcal{I}_r$ may differ according to the fuzzy rules in order to enhance design flexibility. Furthermore, the mismatched disturbance matrix B_{di} with $i \in \mathcal{I}_r$ has a same value regardless of its fuzzy rules, which means that B_{di} follows the form of $B_{d1} = B_{d2} = \cdots = B_{dr}$.

Considering Assumption 2, modifying the fuzzy model (1) into a suitable form for the design of IFSMC is important. Therefore, the following transformation will be applied [24], [34]:

$$\begin{aligned}&\bar{B} = \frac{1}{r}\sum_{i=1}^{r} B_i, \ \bar{V} = \frac{1}{2}\begin{bmatrix}\bar{B} - B_1 & \bar{B} - B_2 & \cdots & \bar{B} - B_r\end{bmatrix},\\ &\bar{U}(\mathbf{w}) = \begin{bmatrix}(1 - 2\,w_1(x(t)))\,I & \cdots & \mathbf{0}\\ \vdots & \ddots & \vdots\\ \mathbf{0} & \cdots & (1 - 2\,w_r(x(t)))\,I\end{bmatrix},\\ &\bar{W} = \begin{bmatrix}I & I & \cdots & I\end{bmatrix}^T,\end{aligned} \tag{5}$$

where the rank of $\bar{B}$ is m (i.e. $\bar{B} \in \mathcal{R}^{n\times m}$ has a full column rank), I is an identity matrix with an appropriate dimension, and $\bar{U}(\mathbf{w})$ is a diagonal matrix composed of normalized membership functions of the fuzzy model (1).

Using the matrices in (5), the following result can be successfully derived:

$$\begin{aligned}&\bar{B} + \bar{V}\bar{U}(\mathbf{w})\bar{W}\\ &= \bar{B} + \frac{1}{2}\left\{(\bar{B} - B_1)(1 - 2w_1(x(t))) + \cdots + (\bar{B} - B_r)\right.\\ &\quad \left.\times (1 - 2w_r(x(t)))\right\}\\ &= \sum_{i=1}^{r} w_i(x(t)) B_i.\end{aligned} \tag{6}$$

Before proceeding, using the properties of $w_i(x(t))$ described in (3), the following inequalities always hold [24]:

$$\begin{cases}\|\bar{U}(\mathbf{w})\| = \|\bar{U}^T(\mathbf{w})\| \le \|I\|,\\ \bar{U}^T(\mathbf{w})\bar{U}(\mathbf{w}) = \bar{U}(\mathbf{w})\bar{U}^T(\mathbf{w}) \le I.\end{cases} \tag{7}$$

Finally, applying the transformation (6), the T–S fuzzy model (2) can be modified as follows:

$$\begin{aligned}\dot{x}(t) &= \sum_{i=1}^{r} w_i(x(t))\left\{A_i x(t) + (\bar{B} + \bar{V}\bar{U}(\mathbf{x})\bar{W})\right.\\ &\quad \left.\times\left[u(t) + H(x(t))\right] + B_{di} d(t)\right\},\\ y(t) &= \sum_{i=1}^{r} w_i(x(t)) C_i x(t).\end{aligned} \tag{8}$$

Additionally, the following lemma is necessary for verification of the proof process throughout this paper.

Lemma 1 [12]: Given the constant matrices D and E, symmetric constant matrix S, and time-varying matrix $F(t)$ with appropriate dimensions, the following matrix inequality always holds for any scalar $\epsilon > 0$ if $F(t)$ satisfies $F^T(t)F(t) \le I$:

$$S + DF(t)E + E^T F^T(t) D^T \le S + \epsilon E^T E + \epsilon^{-1} D D^T. \tag{9}$$

Remark 1: Lemma 1 will be needed because of the modified form (8)*. Unlike conventional T–S fuzzy model approach [5]–[12], [16], the input matrix structure is separated with several matrices, such as* $\bar{B}$, $\bar{V}$, $\bar{U}(\mathbf{w})$, *and* $\bar{W}$. *Given the time-varying matrix* $\bar{U}(\mathbf{w})$, *Lemma 1 will be helpful when deriving a stability analysis of* (8).

B. ANALYSIS OF NON-PERIODIC DISTURBANCE WITH FOURIER APPROACH

In this subsection, we first mention the limitation of DOBC methods described in the previous approaches [16], [17], [20]–[23] and introduce Fourier analysis to deal with this problem. Many previous studies have assumed that the form of mismatched disturbance $d(t)$ is a real-valued periodic signal with a certain frequency and generated through an exogenous system satisfying the following linear differential equation structure [20], [21]:

$$\begin{cases} \dot{\xi}(t) = \bar{A}_d \xi(t), \\ d(t) = \bar{C}_d \xi(t), \end{cases} \tag{10}$$

where $\bar{A}_d \in \mathbb{R}^{2\times 2}$, $\bar{C}_d \in \mathbb{R}^{1\times 2}$ are known constant matrices, and $\xi(t) \in \mathbb{R}^2$ indicates the state vector of the exogenous system. Although the above structure (10) can be successfully applied when $d(t)$ is assumed that it follows a periodic signal (i.e. eigenvalues of matrix $\bar{A}_d$ are pure imaginary eigenvalues), however, aforementioned method can be vulnerable to NPNS signals, and if the form of $d(t)$ does not follow the form of (10), designed DOB may not successfully estimate the $d(t)$. In other words, plants or objects we are trying to control may not fulfill our requirements.

Motivated by the above-mentioned limitation, we will analyze the $d(t)$ with a given time interval and apply Fourier analysis in advance of designing FDOB and controller. The main goal of the proposed method is to apply the structure of the similar form (10) when designing an FDOB and to show the possibility that the NPNS signal can be handled via the previous DOBC concept. By applying the Fourier analysis to the NPNS signal acting on the system, it allows us to filter out several distinct dominant periodic sinusoid (DPS) signals with important features, such as frequency, phase, and magnitude of those signals. After using this information, it is possible to generate artificial sinusoid signals similar to the DPS signals by applying an analogous structure of (10).

To sum up, if we can formulate several FDOBs corresponding to those artificial sinusoid signals respectively, it is possible to estimate dominant portions of the NPNS signal $d(t)$, which indicates that attenuating the influence of $d(t)$ can be successfully achieved by designing several FDOBs.

Instead of using the previous structure (10), a novel form (11) will be applied when designing FDOBs:

$$\begin{cases} \dot{s}_k(t) = \bar{A}_{kd} s_k(t) + B_{wk}\delta(t), \\ d_k(t) = \bar{C}_{kd} s_k(t), \end{cases} \tag{11}$$

where $k \in \mathcal{I}_N$, and N is the number of DPS signals which determine the main characteristics of original NPNS signal $d(t)$. Additionally, $d_k(t) \in \mathcal{R}^1$ is an artificially generated periodic signal, $s_k(t) \in \mathcal{R}^2$ is a state vector of artificial generated system and its initial condition is assumed as $s_k(0) = 0$. Moreover, $\bar{A}_{kd} \in \mathcal{R}^{2\times 2}$, $B_{wk} \in \mathcal{R}^{2\times 1}$, and $\bar{C}_{kd} \in \mathcal{R}^{1\times 2}$ are constant matrices determined after applying Fourier analysis and $\delta(t)$ is a constant function with a value of 1.

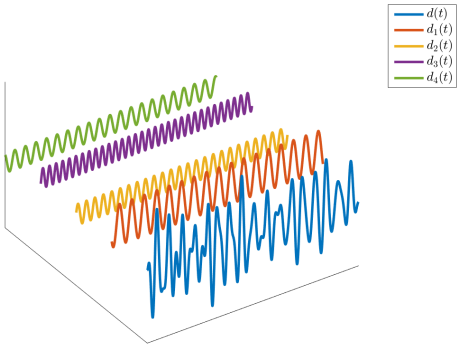

FIGURE 1. Non-periodic neutral stable signal $d(t)$ can be decomposed by several dominant periodic sinusoid signals $d_1(t)$ to $d_4(t)$ via Fourier analysis.

Remark 2: The proposed design procedure can be considered as limited with respect to analyzing the features of $d(t)$ *prior to designing an FDOB and controller. Designing FDOBs and controller without knowledge of* $d(t)$ *is considered as a more ideal case. Even though the proposed method can be regarded as limited, however, it suggests a potential that the proposed method can broaden the perspective that the previous DOBC concept can be enlarged into NPNS signals. The detailed explanation of how the NPNS signal* $d(t)$ *can be generated through the structure of* (11) *is delineated in Appendix B.*

Finally, applying the structure (11), the NPNS disturbance $d(t)$ can be considered as a linear summation of DPS signals as follows:

$$d(t) = d_1(t) + d_2(t) + \cdots + d_N(t) + E_d(t), \tag{12}$$

where $E_d(t) \in \mathbb{R}^1$ is a residual error function which can not be represented by $d_k(t)$ for $k \in \mathcal{I}_N$. Therefore, given the equation (12), the modified T–S fuzzy model (8) can be considered as follows:

$$\begin{aligned} \dot{x}(t) = \sum_{i=1}^{r} w_i(x(t)) \big\{ & A_i x(t) + (\bar{B} + \bar{V}\bar{U}(\mathbf{x})\bar{W}) \\ & \times [u(t) + H(x(t))] + B_{di}(d_1(t) + d_2(t) + \\ & \cdots + d_N(t) + E_d(t)) \big\}, \end{aligned} \tag{13}$$

$$y(t) = \sum_{i=1}^{r} w_i(x(t)) C_i x(t). \tag{14}$$

For example, Fig. 1 shows that an arbitrary NPNS signal $d(t)$ satisfying Assumption 1 can be decomposed by four DPS signals. Given the form of (12), if we formulate several FDOBs corresponding to each DPS signal respectively, combined estimated disturbance signals derived from designed FDOBs will efficiently reduce the effect of $d(t)$ regardless of

the existence of $E_d(t)$. The detailed design process of FDOBs will be covered in the next subsection.

C. FUZZY DISTURBANCE OBSERVER DESIGN

In this subsection, motivated by the original DOB design concept in [20], designing N FDOBs corresponding artificially generated periodic signal $d_k(t)$ for $k \in \mathcal{I}_N$ is presented. The designed FDOB with IF-THEN rules is as follows:

FDOB rule i corresponding $d_k(t)$:
IF $x_1(t)$ is M_1^i and $x_2(t)$ is $M_2^i \cdots$ and $x_z(t)$ is M_z^i,
THEN

$$\begin{cases} \dot{p}_k(t) = (\bar{A}_{kd} - L_k B_{di} \bar{C}_{kd})\hat{s}_k(t) - L_k \{A_i x(t) \\ \quad + (\bar{B} + \bar{V}\bar{U}(\mathbf{w})\bar{W})[u(t) + H(x(t))] \\ \quad + B_{di} D_k(t)\}, \\ \hat{s}_k(t) = p_k(t) + L_k x(t), \\ \hat{d}_k(t) = \bar{C}_{kd}\hat{s}_k(t), \end{cases} \tag{15}$$

where $\hat{s}_k(t) \in \mathcal{R}^2$ denotes the k^{th} estimated state of an artificially generated system (11), $\hat{d}_k(t) \in \mathcal{R}^1$ denotes a k^{th} estimated artificial disturbance, $p_k(t) \in \mathcal{R}^2$ stands for an internal state vector of k^{th} FDOB, and $L_k \in \mathcal{R}^{2\times 2}$ stands for k^{th} FDOB gain matrix, which will be determined later. Moreover, $D_k(t)$ satisfies the following equations.

$$\begin{cases} D_1(t) = d_2(t) + d_3(t) + \cdots + d_N(t) + E_d(t), \\ D_2(t) = d_1(t) + d_3(t) + \cdots + d_N(t) + E_d(t), \\ \vdots \\ D_N(t) = d_1(t) + d_2(t) + \cdots + d_{N-1}(t) + E_d(t). \end{cases}$$

For simplicity, we assume that $\hat{s}_k(0) = 0$ and $\hat{d}_k(0) = 0$. Using the same procedure applied in (2), the fuzzified equation (15) is obtained as follows:

$$\begin{aligned} \dot{p}_k(t) &= \sum_{i=1}^{r} w_i(x(t)) \{(\bar{A}_{kd} - L_k B_{di}\bar{C}_{kd})\hat{s}_k(t) \\ &\quad - L_k\{A_i x(t) + (\bar{B} + \bar{V}\bar{U}(\mathbf{w})\bar{W}) \\ &\quad \times [u(t) + H(x(t))] + B_{di} D_k(t)\}\}, \\ \hat{s}_k(t) &= p_k(t) + L_k x(t), \\ \hat{d}_k(t) &= \bar{C}_{kd}\hat{s}_k(t). \end{aligned} \tag{16}$$

Subsequently, we can define a state error vector $\tilde{s}_k(t)$ as follows:

$$\tilde{s}_k(t) = s_k(t) - \hat{s}_k(t). \tag{17}$$

Applying the above equations (8), (11), (16), and (17), we can derive the following differential equation in terms of $\tilde{s}_k(t)$ as follows:

$$\begin{aligned} \dot{\tilde{s}}_k(t) &= \dot{s}_k(t) - \dot{\hat{s}}_k(t) \\ &= \bar{A}_{kd} s_k(t) + B_{wk}\delta(t) - \dot{p}_k(t) - L_k \dot{x}(t) \\ &= \sum_{i=1}^{r} w_i(x(t)) \left\{(\bar{A}_{kd} - L_k B_{di}\bar{C}_{kd})\tilde{s}_k(t) + B_{wk}\delta(t)\right\}. \end{aligned} \tag{18}$$

Remark 3: The form of (18) *implies that if we can determine the FDOB gain matrix L_k with $k \in \mathcal{I}_N$ making* (18) *as an asymptotically stable, the estimated value $\hat{s}_k(t)$ will successfully follow the real value $s_k(t)$.*

D. INTEGRAL FUZZY SLIDING MODE CONTROL

In this subsection, the design procedure of IFSMC stabilizing the modified T–S fuzzy model (8) is proposed. The designed IFSMC can successfully reduce the effect of $H(x(t))$ and $d(t)$ simultaneously. To design IFSMC, the following control law will be applied [18, eq.(7)]:

$$u(t) = u_o(t) + u_n(t), \tag{19}$$

where $u_o(t)$ denotes a nominal control input with proper feedback, and $u_n(t)$ denotes a discontinuous part to induce a sliding mode.

The nominal control input with proper feedback via parallel distributed compensation (PDC) method [16] is as follows:

Nominal controller rule j :
IF $x_1(t)$ is M_1^j and $x_2(t)$ is $M_2^j \cdots$ and $x_z(t)$ is M_z^j,
THEN $u_o(t) = K_j x(t) - K_{dj}\hat{d}(t)$. (20)

Moreover, $K_j \in \mathcal{R}^{m\times n}$, $K_{dj} = \bar{B}^+ B_{dj} \in \mathcal{R}^{m\times 1}$, where $\bar{B}^+ = (\bar{B}^T\bar{B})^{-1}\bar{B}^T$, represent feedback control and disturbance compensation gain matrices for the jth rule. Additionally, the value of $\hat{d}(t)$ is a result of combination $\hat{d}_1(t) + \hat{d}_2(t) + \cdots + \hat{d}_N(t)$.

Finally, using the same procedure applied in (2), the inferred result of the nominal controller $u_o(t)$ is obtained as follows:

$$u_o(t) = \sum_{i=1}^{r} w_i(x(t)) \left\{K_j x(t) - K_{dj}\hat{d}(t)\right\}. \tag{21}$$

Remark 4: Before proceeding, the notation for normalized membership function $w_i(x(t))$, and matrix $\bar{U}(\mathbf{w})$ are denoted as w_i and $\bar{U}$ for simplicity.

Next, a novel sliding surface $\mathcal{S}(t) \in \mathcal{R}^m$ combined with estimated sum of disturbance $\hat{d}(t)$ is proposed as follows:

$$\begin{aligned} \mathcal{S}(t) = G \Bigg\{ (x(t) - x(0)) - \int_0^t \sum_{i=1}^{r} w_i \{A_i x(\tau) \\ + (\bar{B} + \bar{V}\bar{U}\bar{W})u_o(\tau) + B_{di}\hat{d}(\tau)\} d\tau \Bigg\}, \end{aligned} \tag{22}$$

where $G \in \mathcal{R}^{m\times n}$ denotes a sliding surface decision variable, which will be determined later.

To derive a sliding dynamic, an equivalent control concept is applied [18, eq.(9)]. Considering the necessary condition for the sliding dynamic $\mathcal{S}(t) = 0$ and $\dot{\mathcal{S}}(t) = 0$, the derivative of the sliding surface $\mathcal{S}(t)$ with respect to time t can be

represented by referring (13):

$$\begin{aligned}\dot{\mathcal{S}}(t) &= G\left\{\dot{x}(t) - \sum_{i=1}^{r} w_i\{A_i x(t) + (\bar{B} + \bar{V}\bar{U}\bar{W})u_o(t) \right. \\ &\quad \left. + B_{di}\hat{d}(t)\}\right\} \\ &= \sum_{i=1}^{r} w_i G\left\{(\bar{B} + \bar{V}\bar{U}\bar{W})u_n(t) + (\bar{B} + \bar{V}\bar{U}\bar{W}) \right. \\ &\quad \left. \times H(x(t)) + B_{di}\tilde{d}(t) + B_{di}E_d(t)\right\}. \end{aligned} \tag{23}$$

To satisfy the above condition $\dot{\mathcal{S}}(t) = 0$, the following equation should be satisfied:

$$\begin{aligned}&\sum_{i=1}^{r} w_i G(\bar{B} + \bar{V}\bar{U}\bar{W})u_n^{eq}(t) \\ &= -\sum_{i=1}^{r} w_i G\left\{(\bar{B} + \bar{V}\bar{U}\bar{W})H(x(t)) + B_{di}(\tilde{d}(t) + E_d(t))\right\},\end{aligned} \tag{24}$$

where $u_n^{\mathrm{eq}}(t)$ is an equivalent control law for the discontinuous part.

Next, simplified expression of (24) is given as follows:

$$\begin{aligned}Tu_n^{\mathrm{eq}}(t) &= -TH(x(t)) - \sum_{i=1}^{r} w_i G B_{di}\tilde{d}(t) \\ &\quad - \sum_{i=1}^{r} w_i G B_{di}E_d(t),\end{aligned} \tag{25}$$

where

$$T \in \mathcal{R}^{m\times m} = \sum_{i=1}^{r} w_i G(\bar{B} + \bar{V}\bar{U}\bar{W}) = G(\bar{B} + \bar{V}\bar{U}\bar{W}).$$

To derive $u_n^{\mathrm{eq}}(t)$ properly, determining whether T is a non-singular or not should be considered at first. Given this point, the following lemma [24], [34, Lemma 4] will be applied:

Lemma 2: [24], [34] Consider the following LMIs:

$$\begin{bmatrix} -I & * \\ c_1\bar{V} & -I \end{bmatrix} < 0, \quad \begin{bmatrix} Q & * \\ I & c_2 I \end{bmatrix} > 0, \quad Q < c_3 I,$$
$$\begin{bmatrix} 2\,c_1\sqrt{\lambda_{min}(\bar{B}^T\bar{B})} & * & * \\ rc_2 & rc_1 & * \\ rc_3 & 0 & rc_1 \end{bmatrix} > 0, \tag{26}$$

where $Q \in \mathcal{R}^{n\times n}$, $c_1 \in \mathcal{R}^1$, $c_2 \in \mathcal{R}^1$, and $c_3 \in \mathcal{R}^1$ are decision variables with $Q > 0$. If LMIs in (26) are satisfied, then there exist a matrix $G = (\bar{B}^T Q^{-1}\bar{B})^{-1}\bar{B}^T Q^{-1}$ such that $T = G(\bar{B} + \bar{V}\bar{U}\bar{W})$ makes a non-singular.

If Lemma 2 is satisfied, and decision variables are successfully determined, then we can multiply T^{-1} both sides of the (25). As a result, the following equivalent control law $u_n^{\mathrm{eq}}(t)$ can be successfully derived:

$$\begin{aligned}u_n^{\mathrm{eq}}(t) &= -H(x(t)) - \sum_{i=1}^{r} w_i T^{-1} G B_{di}\tilde{d}(t) \\ &\quad - \sum_{i=1}^{r} w_i T^{-1} G B_{di}E_d(t).\end{aligned} \tag{27}$$

Before proceeding, it is important to remind that the possibility of invertible of the matrix T is revealed through Lemma 2, however, finding an upper bound of T^{-1} and $(T^{-1})^T$ is necessary in order to successfully derive the stability of sliding dynamic. Therefore, the following lemma is proposed:

Lemma 3: Provided that Lemma 2 is successfully satisfied. Then the non-singular matrix T satisfies the following inequalities:

$$\|T^{-1}\| \le p_1, \quad \|(T^{-1})^T\| \le p_2, \tag{28}$$

where

$$p_1 = \|I\| + \|G\bar{V}\|\|\bar{W}\|, \;\; p_2 = \|I\| + \|\bar{W}^T\|\|\bar{V}^T G^T\|.$$

Proof: First, we will derive $\|T^{-1}\| \le p_1$. Assuming that Lemma 2 is satisfied and sliding surface decision variable G is successfully determined, then T is a non-singular matrix and can be represented as follows:

$$T = G\bar{B} + G\bar{V}\bar{U}\bar{W} = I + G\bar{V}\bar{U}\bar{W}.$$

Moreover, the following inequalities are always satisfied [31]:

$$\begin{aligned}\|T\| &= \|I + G\bar{V}\bar{U}\bar{W}\| \le \|I\| + \|G\bar{V}\bar{U}\bar{W}\|, \\ \|T\|^{-1} &= \left(\|I + G\bar{V}\bar{U}\bar{W}\|\right)^{-1} \ge \left(\|I\| + \|G\bar{V}\bar{U}\bar{W}\|\right)^{-1}.\end{aligned}$$

Next, using a property $\|T^{-1}\| \ge \|T\|^{-1}$, the following result can be derived:

$$\left(\|I\| + \|G\bar{V}\bar{U}\bar{W}\|\right)^{-1} \le \|T^{-1}\| \le \|I\| + \|G\bar{V}\bar{U}\bar{W}\|.$$

By applying the above result, an upper bound of $\|T^{-1}\|$ can be represented as follows:

$$\|T^{-1}\| \le \|I\| + \|G\bar{V}\bar{U}\bar{W}\|. \tag{29}$$

Moreover, if we apply the first inequality condition in (7), then (29) can be represented as follows:

$$\|T^{-1}\| \le \|I\| + \|G\bar{V}\bar{U}\bar{W}\| \le \|I\| + \|G\bar{V}\|\|\bar{W}\| = p_1.$$

Then the proof of $\|T^{-1}\| \le p_1$ is complete.

Second, the proof of $\|(T^{-1})^T\| \le p_2$ can be similarly induced to the former approach. The transpose of the matrix T is obtained as follows:

$$T^T = I + \bar{W}^T\bar{U}^T\bar{V}^T G^T.$$

Moreover, the following inequalities always hold in order:

$$\begin{aligned}\|T^T\| &\le \|I\| + \|\bar{W}^T\bar{U}^T\bar{V}^T G^T\|, \\ \|T^T\|^{-1} &\ge \left(\|I\| + \|\bar{W}^T\bar{U}^T\bar{V}^T G^T\|\right)^{-1}.\end{aligned}$$

Next, applying properties $\|\left(T^T\right)^{-1}\| \ge \|T^T\|^{-1}$ and $\left(T^T\right)^{-1} = \left(T^{-1}\right)^T$, the following inequality is obtained:

$$\|\left(T^T\right)^{-1}\| = \|\left(T^{-1}\right)^T\| \ge \left(\|I\| + \|\bar{W}^T\bar{U}^T\bar{V}^T G^T\|\right)^{-1}.$$

Moreover, by applying the above result and first inequality in (7), an upper bound of $\|\left(T^{-1}\right)^T\|$ can be formulated as follows:

$$\begin{aligned}\|\left(T^{-1}\right)^T\| &\leq \|I\| + \|\bar{W}^T\bar{U}^T\bar{V}^T G^T\| \\ &\leq \|I\| + \|\bar{W}^T\|\|\bar{V}^T G^T\| = p_2.\end{aligned}$$

Finally, the proof of Lemma 3 is completed. □

Remark 5: In fact, considering the form of p_1 and p_2 in Lemma 3, the values of p_1 and p_2 are the same. For simplicity, in the rest of the paper, the notation for p_1 and p_2 will be unified as p_1.

Next step, we can substitute $u_n^{\text{eq}}(t)$ from (27) and $u_o(t)$ from (21) into the modified form (8). Therefore, sliding dynamic equations can be derived as follows:

$$\begin{aligned}\dot{x}(t) = &\sum_{i=1}^{r}\sum_{j=1}^{r} w_i w_j \Big\{(A_i + \bar{B}K_j)x(t) + \bar{B}K_{dj}\tilde{d}(t) \\ &+ (B_{di} - \bar{B}K_{dj})d(t) - \bar{B}T^{-1}GB_{dj}(\tilde{d}(t) + E_d(t)) \\ &+ \bar{\Delta}K_j x(t) + (\bar{\Delta}K_{dj} - \bar{\Delta}T^{-1}GB_{dj})\tilde{d}(t) - \bar{\Delta}T^{-1} \\ &\times GB_{dj}E_d(t) - \bar{\Delta}K_{dj}d(t)\Big\}, \\ y(t) = &\sum_{i=1}^{r} w_i x(t),\end{aligned} \tag{30}$$

where $\bar{\Delta} = \bar{V}\bar{U}\bar{W}$, $T^{-1} = \left(G(\bar{B} + \bar{V}\bar{U}\bar{W})\right)^{-1}$.

Before analyzing the stability of (30), augmenting (18) and (30) yields the following state-space representation:

$$\begin{aligned}\dot{\bar{x}}(t) = &\sum_{i=1}^{r}\sum_{j=1}^{r} w_i w_j \left\{\mathcal{A}_{ij}\bar{x}(t) + \mathcal{D}_{ij}d(t) + \mathcal{B}_w\delta(t)\right. \\ &\left. + \Delta_{1j}x(t) - \Delta_{2j}d(t) + \Delta_{3j}\tilde{d}(t) - \Delta_{4j}E_d(t)\right\}, \\ y(t) = &\sum_{i=1}^{r} w_i \mathcal{C}_i\bar{x}(t),\end{aligned} \tag{31}$$

where detailed descriptions are presented at (32), as shown at the bottom of the page.

Furthermore, to satisfy an H_∞ control performance of the sliding dynamic, the following problem is considered:

Problem 1 [16]: For a predefined positive scalar $\gamma > 0$, we design the sliding dynamic (31) such that the following conditions are satisfied:

(1) The sliding dynamic (31) under $\bar{d}(t) = 0$ is asymptotically stable.

(2) Under the zero initial condition, the sliding dynamic (31) satisfies the following condition:

$$\lim_{t\to\infty} \psi(t) \leq \gamma^2, \tag{33}$$

where

$$\psi(t) = \frac{\int_0^t y^T(\tau)y(\tau)d\tau}{\int_0^t \bar{d}^T(\tau)\bar{d}(\tau)d\tau},$$
$$\bar{d}(t) = \begin{bmatrix} d^T(t) & E_d^T(t) & \delta^T(t)\end{bmatrix}^T.$$

III. MAIN RESULT

A. DERIVING A STABILIZATION CONDITION OF SLIDING DYNAMIC

In this subsection, an LMI-based condition for asymptotic stability with H_∞ control performance on the sliding dynamic is proposed.

Theorem 1: For a given scalar $\gamma > 0$, proper scalar α_k with $k \in \mathcal{I}_4$, and predefined design parameter N, the sliding dynamic of the T–S fuzzy model (31) is asymptotically stable with H_∞ control performance addressed in Problem 1, if there exist matrices $X = X^T \in \mathcal{R}^{n\times n}$, $P_k \in \mathcal{R}^{2\times 2}$, $Y_k \in \mathcal{R}^{2\times 2}$ for $k \in \mathcal{I}_N$, and $N_j \in \mathcal{R}^{m\times n}$ for $j \in \mathcal{I}_r$ such that the following LMIs are satisfied:

$$X > 0, \tag{34}$$
$$P_k > 0, \quad k \in \mathcal{I}_N, \tag{35}$$
$$\Theta_{ii} > 0, \quad i \in \mathcal{I}_r, \tag{36}$$
$$\Theta_{ij} + \Theta_{ji} < 0, \quad i < j \in \mathcal{I}_r, \tag{37}$$

where detailed description for Θ_{ij} with $i, j \in \mathcal{I}_r$ is represented in (66). Finally, feedback control gain matrices and FDOB gain matrices are obtained as $K_j = N_j X^{-1}$, $L_k = P_k^{-1}Y_k$.

Proof: For the efficient placement of the paper, the detailed proof of Theorem 1 is provided in Appendix A. □

In the process of designing a sliding mode controller, the problem of reachability of the sliding dynamic also should be addressed. Before proceeding, the following lemmas are useful when deriving the reachability problem.

Lemma 4 [16], [23]: We assume $\bar{A} \in \mathcal{R}^{n\times n}$ is Hurwitz (i.e. the real parts of eigenvalues of $\bar{A}$ are negative), and thus there exists a scalar $\xi > 0$ such that $\|e^{\bar{A}t}\| \leq \xi e^{\frac{\lambda_{max}(\bar{A})}{2}t}$.

$$\mathcal{A}_{ij} = \begin{bmatrix} A_i + \bar{B}K_j & \Gamma_j\bar{C}_{1d} & \cdots & \Gamma_j\bar{C}_{Nd} \\ \mathbf{0} & \bar{A}_{1d} - L_1B_{di}\bar{C}_{1d} & \cdots & \mathbf{0} \\ \vdots & \vdots & \ddots & \vdots \\ \mathbf{0} & \mathbf{0} & \cdots & \bar{A}_{Nd} - L_NB_{di}\bar{C}_{Nd}\end{bmatrix}, \ \bar{x}(t) = \begin{bmatrix} x(t) \\ \bar{s}(t)\end{bmatrix}, \ \bar{s}(t) = \begin{bmatrix} \tilde{s}_1(t) \\ \vdots \\ \tilde{s}_N(t)\end{bmatrix}, \mathcal{C}_i = \begin{bmatrix} C_i & \mathbf{0}\end{bmatrix},$$
$$\mathcal{D}_{ij} = \begin{bmatrix}(B_{di} - \bar{B}K_{dj})^T & \mathbf{0}\end{bmatrix}^T, \ \mathcal{B}_w = \begin{bmatrix}\mathbf{0} & B_{w1}^T\ q\cdots & B_{wN}^T\end{bmatrix}^T, \ \Delta_{1j} = \begin{bmatrix}(\bar{\Delta}K_j)^T & \mathbf{0}\end{bmatrix}^T, \ \Delta_{2j} = \begin{bmatrix}(\bar{\Delta}K_{dj})^T & \mathbf{0}\end{bmatrix}^T,$$
$$\Delta_{3j} = \begin{bmatrix}(\bar{\Delta}K_{dj} - \bar{\Delta}T^{-1}GB_{dj} - \bar{B}T^{-1}GB_{dj})^T\ \mathbf{0}\end{bmatrix}^T, \ \Delta_{4j} = \begin{bmatrix}(\bar{\Delta}T^{-1}GB_{dj} + \bar{B}T^{-1}GB_{dj})^T & \mathbf{0}\end{bmatrix}^T, \ \Gamma_j = \bar{B}K_{dj}, \tag{32}$$

where $\mathbf{0}$ denotes a zero matrix with an appropriate dimension.

Lemma 5: Considering designed FDOBs, the artificial exogenous system state error $\tilde{s}_k(t)$ with $k \in \mathcal{I}_N$ satisfies the following condition:

$$\|\tilde{s}_k(t)\| \leq \upsilon_k, \tag{38}$$

where υ_k is a positive scalar.

Proof: Before verifying Lemma 5, recall the following equation in terms of artificial exogenous state error vector $\tilde{s}_k(t)$ with $k \in \mathcal{I}_N$.

$$\dot{\tilde{s}}_k(t) = \textstyle\sum_{i=1}^{r} w_i \left\{(\bar{A}_{kd} - L_k B_{di} \bar{C}_{kd})\tilde{s}_k(t) + B_{wk}\delta(t)\right\}.$$

To derive (38), representing the general solution of $\tilde{s}_k(t)$ is necessary. Thus, the following result can be obtained:

$$\tilde{s}_k(t) = e^{\Lambda_k t}\tilde{s}_k(0) + \textstyle\int_0^t e^{\Lambda_k(t-\tau)} B_{wk}\delta(\tau)d\tau, \tag{39}$$

where

$$\Lambda_k = \sum_{i=1}^{r} w_i \left\{\bar{A}_{kd} - L_k B_{di}\bar{C}_{kd}\right\}, \ k \in \mathcal{I}_N.$$

Considering the condition $\hat{s}_k(0) = 0$ and $s_k(0) = 0$, the initial value of $\tilde{s}_k(t)$ can be regarded as zero. Additionally, if FDOB gain matrix L_k is successfully determined through Theorem 1, then Λ_k is said to be a Hurwitz. Therefore, Lemma 4 can be applied to Λ_k.

Referring Lemma 4 and (39), the following inequalities can be successfully obtained:

$$\begin{aligned}
\|\tilde{s}_k(t)\| &\leq \|e^{\Lambda_k t}\tilde{s}_k(0)\| + \|\int_0^t e^{\Lambda_k(t-\tau)} B_{wk}\delta(\tau)d\tau\| \\
&= \|\int_0^t e^{\Lambda_k(t-\tau)} B_{wk}\delta(\tau)d\tau\| \\
&\leq \|B_{wk}\| \int_0^t \|e^{\Lambda_k(t-\tau)}\| d\tau \\
&\leq \xi\|B_{wk}\| \int_0^t e^{\frac{\lambda_{\max}(\Lambda_k)}{2}(t-\tau)} d\tau \\
&\leq -\xi\|B_{wk}\| \frac{2}{\lambda_{\max}(\Lambda_k)} \left(1 - e^{\frac{\lambda_{\max}(\Lambda_k)t}{2}}\right) \\
&\leq \frac{-2\xi\|B_{wk}\|}{\lambda_{\max}(\Lambda_k)} = \upsilon_k,
\end{aligned} \tag{40}$$

where $\upsilon_k = \frac{-2\xi\|B_{wk}\|}{\lambda_{\max}(\Lambda_k)}$. Therefore, it proves that the artificial exogenous system state error $\tilde{s}_k(t)$ for $k \in \mathcal{I}_N$ is norm bounded, thus, it is ready for deriving a reachability problem of the designed sliding surface $\mathcal{S}(t)$ successfully. The reachability problem will be delineated in the next subsection. □

B. REACHABILITY ANALYSIS

In this subsection, the reachability problem for the designed sliding surface $\mathcal{S}(t)$ will be addressed by applying a proper Lyapunov function.

Theorem 2: Using the fuzzy sliding mode controller (41), the state trajectories of the T–S fuzzy model (8) are successfully reached on the proposed sliding surface $\mathcal{S}(t) = 0$.

$$u(t) = \sum_{j=1}^{r} w_j \left\{K_j x(t) - K_{dj}\hat{d}(t) + u_n(t)\right\}, \tag{41}$$

where

$$\begin{aligned}
u_n(t) &= -\sigma(t)sgn(\mathcal{S}(t)), \\
\sigma(t) &= \eta + \epsilon\|x(t)\| + p_1(|M| + \alpha)\|\sum_{i=1}^{r} w_i G B_{di}\|, \\
M &= \bar{C}_{1d}\upsilon_1 + \cdots + \bar{C}_{Nd}\upsilon_N.
\end{aligned}$$

Moreover, η corresponds to a small scalar.

Proof: To derive the reachability problem, the derivative of $\mathcal{S}(t)$ with respect to time t is needed. Recall the previous result (23) as follows:

$$\dot{\mathcal{S}}(t) = Tu_n(t) + TH(x(t)) + \sum_{i=1}^{r} w_i G B_{di}\left(\tilde{d}(t) + E_d(t)\right).$$

Next, consider the following Lyapunov candidate function:

$$V_R(\mathcal{S}(t)) = \frac{1}{2}\mathcal{S}^T(t)\mathcal{S}(t). \tag{42}$$

The derivative of $V_R(\mathcal{S}(t))$ with respect to time t can be obtained by referring to $\dot{\mathcal{S}}(t)$:

$$\begin{aligned}
\dot{V}_R(\mathcal{S}(t)) &= \mathcal{S}^T(t)\dot{\mathcal{S}}(t) \\
&= \mathcal{S}^T(t)\{-T\sigma(t)\mathrm{sgn}(\mathcal{S}(t)) + TH(x(t)) \\
&\quad + \sum_{i=1}^{r} w_i G B_{di}(\tilde{d}(t) + E_d(t))\}.
\end{aligned} \tag{43}$$

In addition, the following inequalities can be obtained considering Assumption 1 and Lemma 3:

$$\begin{aligned}
\dot{V}_R(\mathcal{S}(t)) &\leq \|\mathcal{S}^T(t)\|\{-T\sigma(t) + TH(x(t)) + \sum_{i=1}^{r} w_i G B_{di} \\
&\quad \times (\tilde{d}(t) + E_d(t))\} \\
&\leq \|\mathcal{S}^T(t)\|\|T\|\{-\sigma(t) + \epsilon\|x(t)\| + p_1(|M| + \alpha) \\
&\quad \times \|\sum_{i=1}^{r} w_i G B_{di}\|\}.
\end{aligned} \tag{44}$$

Next, substitute $\sigma(t)$ presented in Theorem 2 into (44), we have the following:

$$\dot{V}_R(\mathcal{S}(t)) \leq -\eta\|\mathcal{S}^T(t)\|\|T\| \leq 0. \tag{45}$$

Therefore, if we properly choose the value of η, then the state trajectories of (8) can reach the proposed sliding surface $\mathcal{S}(t) = 0$. Finally, the proof of Theorem 2 is completed. □

Remark 6 [26]: It is necessary to remember that discontinuous control term $u_n(t)$ in the designed fuzzy sliding mode controller (41) can give rise to a chattering problem when reaching onto the sliding surface $\mathcal{S}(t) = 0$. This problem can be relaxed by replacing the term $sgn(\mathcal{S}(t))$ into $\frac{\mathcal{S}(t)}{|\mathcal{S}(t)|+\theta}$, where θ is a small scalar.

Remark 7: The design parameter N in $u(t)$ has some trade-offs to be considered. If the number of N is big, the influence of $d(t)$ will be attenuated significantly because formulated FDOBs as the same number of N can estimate the dominant portions of $d(t)$. Although the influence of $d(t)$ may successfully decrease, however, the entire costs for formulating several FDOBs will be increased. Considering the above trade-off should be noted before designing a controller.

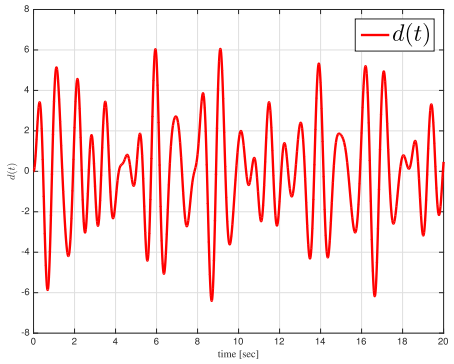

(a)

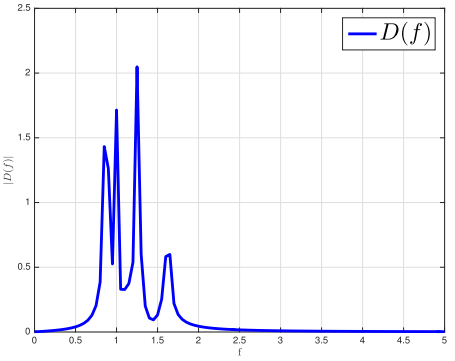

(b)

FIGURE 2. (a) Trajectory of the NPNS disturbance $d(t)$ for time interval 0s to 20s; (b) the Fourier coefficient $D(f)$ of $d(t)$.

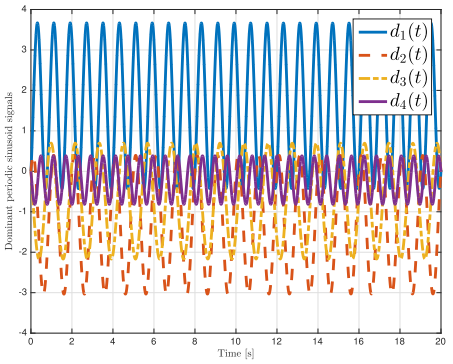

(a)

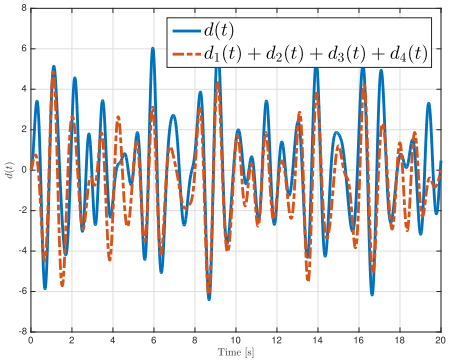

(b)

FIGURE 3. (a) Trajectories of the dominant periodic sinusoid signals comprising $d(t)$; (b) trajectories of the NPNS disturbance $d(t)$ (solid) and summation of dominant periodic signals (dashed).

IV. SIMULATION RESULTS

In this section, simulation will be conducted on the inverted pendulum system because its T–S fuzzy model has different input matrices corresponding its fuzzy rules, which means that it is a good testbed for taking simulation.

Consider the following T–S fuzzy model based inverted pendulum system [28], [29]:

$$\begin{aligned}\dot{x}(t) &= \sum_{i=1}^{4} w_i \left\{A_i x(t) + B_i[u(t) + H(x(t))] + B_{di} d(t)\right\},\\ y(t) &= \sum_{i=1}^{4} w_i C_i x(t),\end{aligned} \tag{46}$$

where system matrices are given as follows:

$$\begin{cases} A_1 = A_2 = \begin{bmatrix} 0 & 1 \\ 10.1385 & 0 \end{bmatrix}, A_3 = A_4 = \begin{bmatrix} 0 & 1 \\ 17.7767 & 0 \end{bmatrix}, \\ B_1 = B_3 = \begin{bmatrix} 0 \\ -0.1395 \end{bmatrix}, B_2 = B_4 = \begin{bmatrix} 0 \\ -0.0302 \end{bmatrix}, \\ C_k = \begin{bmatrix} 1 & 0 \end{bmatrix}, B_{dk} = \begin{bmatrix} 0 \\ 1 \end{bmatrix}, k \in \mathcal{I}_4. \end{cases}$$

Moreover, it is assumed that a matched disturbance $H(x(t)) = 0.1(4x_1^2(t) + 2x_2(t))$ and NPNS mismatched disturbance $d(t)$, as shown in Fig. 2 (a), are acting on the system (46). Additionally, the T–S fuzzy model (46) can be successfully modified into the same form of (8).

As shown in Fig. 2 (a), the form of $d(t)$ is different from previous studies [16], [17], [20]–[23], which assumed that $d(t)$ follows a periodic sinusoid function. Considering this point, the previous studies can be limited in that designed FDOB and controller may not successfully attenuate the influence of $d(t)$. Given the form of $d(t)$, Fourier analysis allows us to reformulate the $d(t)$ into several DPS signals. For instance, Fig. 2 (b) shows the Fourier coefficient $D(f)$ of the original signal $d(t)$. By considering the magnitude of $D(f)$, $d(t)$ can be thought that it mainly has four DPS signals consisting of that signal, which means that a design parameter N can be determined as 4.

Moreover, Fig. 3 (a) shows each DPS signal and original and Fig. 3 (b) demonstrates that the summation of four DPS signals in Fig. 3 (a) approximately similar to that original signal $d(t)$. The above-mentioned procedure implies that if four FDOBs corresponding each DPS signal $d_k(t)$ for $k \in \mathcal{I}_4$ are formulated properly, the influence of $d(t)$ on the system (13) can be significantly reduced.

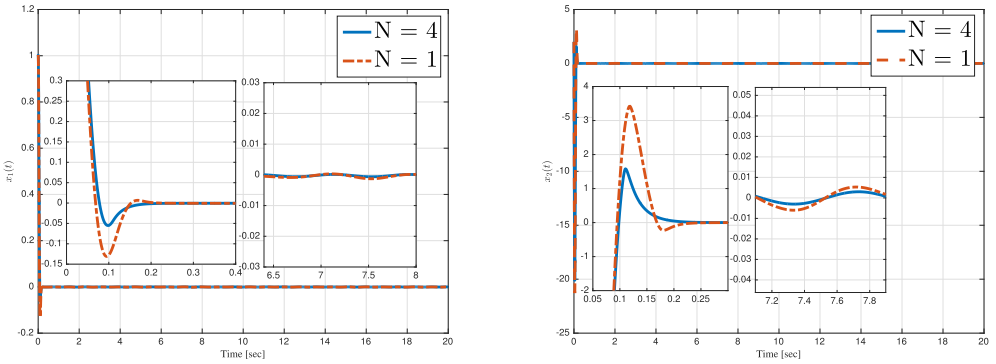

(a) (b)

FIGURE 4. (a) Comparison of state response $x_1(t)$ when $N = 4$ (solid) and $N = 1$ (dashed); (b) comparison of state response $x_2(t)$ when $N = 4$ (solid) and $N = 1$ (dashed).

Referring to Appendix B, differential equations generating DPS signals $d_k(t)$ can be obtained as follows:

$$\dot{s}_1(t) = \bar{A}_{1d}s_1(t) + B_{w1}\delta(t),\ d_1(t) = \bar{C}_{1d}s_1(t), \quad (47)$$
$$\dot{s}_2(t) = \bar{A}_{2d}s_2(t) + B_{w2}\delta(t),\ d_2(t) = \bar{C}_{2d}s_2(t), \quad (48)$$
$$\dot{s}_3(t) = \bar{A}_{3d}s_3(t) + B_{w3}\delta(t),\ d_3(t) = \bar{C}_{3d}s_3(t), \quad (49)$$
$$\dot{s}_4(t) = \bar{A}_{4d}s_4(t) + B_{w4}\delta(t),\ d_4(t) = \bar{C}_{4d}s_4(t), \quad (50)$$

where

$$\bar{A}_{1d} = \begin{bmatrix} 0 & 7.85 \\ -7.85 & 0 \end{bmatrix},\ \bar{A}_{2d} = \begin{bmatrix} 0 & 6.28 \\ -6.28 & 0 \end{bmatrix},$$
$$\bar{A}_{3d} = \begin{bmatrix} 0 & 5.34 \\ -5.34 & 0 \end{bmatrix},\ \bar{A}_{4d} = \begin{bmatrix} 0 & 10.36 \\ -10.36 & 0 \end{bmatrix},$$
$$B_{w1} = \begin{bmatrix} 0.61 \\ 0.79 \end{bmatrix}, B_{w2} = \begin{bmatrix} 0.63 \\ -0.76 \end{bmatrix}, B_{w3} = \begin{bmatrix} -0.85 \\ -0.51 \end{bmatrix},$$
$$B_{w4} = \begin{bmatrix} -0.93 \\ -0.36 \end{bmatrix}, \bar{C}_{1d} = \begin{bmatrix} 16.08 & 0 \end{bmatrix}, \bar{C}_{2d} = \begin{bmatrix} 10.77 & 0 \end{bmatrix},$$
$$\bar{C}_{3d} = \begin{bmatrix} 7.64 & 0 \end{bmatrix}, \bar{C}_{4d} = \begin{bmatrix} 6.21 & 0 \end{bmatrix}.$$

Before designing an IFSMC, a sliding surface decision variable matrix G should be initially determined. Applying Lemma 2, decision variables and matrix G, which makes $G(\bar{B} + \bar{V}\bar{U}\bar{W})$ as a non-singular, are determined as follows:

$$c_1 = 10.4479,\ c_2 = 1.2471,\ c_3 = 1.6489,$$
$$Q = \begin{bmatrix} 1.1952 & -0.0002 \\ -0.0002 & 1.1951 \end{bmatrix},\ G = \begin{bmatrix} -0.0015 & -11.1732 \end{bmatrix}.$$

By applying Theorem 1 and solving associated LMIs (34) to (37), controller gain matrix K_j for $j \in \mathcal{I}_4$ and FDOB gain matrix L_k for $k \in \mathcal{I}_4$ are obtained when predefined scalar values γ and α_k for $k \in \mathcal{I}_4$ are set as follows:

$$\begin{cases} \alpha_1 = 1 \times 10^{-7},\ \alpha_2 = 1.75 \times 10^{-6}, \gamma = 0.6, \\ \alpha_3 = 5.174 \times 10^{-6},\ \alpha_4 = 2.174 \times 10^{-5}, \end{cases}$$

$$\begin{cases} K_1 = K_2 = \begin{bmatrix} 14703 & 389 \end{bmatrix}, \\ K_3 = K_4 = \begin{bmatrix} 14789 & 389 \end{bmatrix}, \\ L_1 = \begin{bmatrix} 0 & 7.9717 \\ 0 & 9.8556 \end{bmatrix}, L_2 = \begin{bmatrix} 0 & 19.3619 \\ 0 & 56.9476 \end{bmatrix}, \\ L_3 = \begin{bmatrix} 0 & 16.3036 \\ 0 & 9.0789 \end{bmatrix}, L_4 = \begin{bmatrix} 0 & 10.0287 \\ 0 & 4.7427 \end{bmatrix}. \end{cases}$$

Moreover, controller design parameters in (41) are provided as follows:

$$\eta = 10,\ \epsilon = 3,\ M = 81.75,\ p_1 = 2.1173,\ \alpha = 8.$$

All simulations were run for a given time interval $t \in [0s\ 20s]$. To verify the effectiveness of sifting out DPS signals as possible, simulations will initially proceed by setting $N = 1$, (i.e. using the most dominant signal (47)), and $N = 4$, (i.e. using all DPS signals (47) to (50)) to compare their control performance. After then, previous studies [6, Th.14], [13] and [17] which have proposed robust control techniques by handling disturbances will be conducted together to demonstrate the efficacy of the proposed method when design parameter $N = 4$. Additionally, initial values of the state variables $x(t) = \begin{bmatrix} x_1^T(t)\ x_2^T(t) \end{bmatrix}^T$ were set as $x(0) = \begin{bmatrix} 1\ 2 \end{bmatrix}^T$, and initial values of FDOBs state variables $p_k(t)$ for $k \in \mathcal{I}_4$ are set as $p_k(0) = -L_k x(0)$ to satisfy $\hat{s}_k(0) = 0$ and $\hat{d}_k(0) = 0$.

First, Fig. 4 shows that designing FDOBs considering four DPS signals (47) to (50) gives rise to a better control performance than considering only one DPS signal (47), which implies that estimated disturbance signals from four FDOBs can efficiently reduce the influence of external disturbance $d(t)$. Secondly, Fig. 5 shows that responses of state variables $x_1(t)$ and $x_2(t)$ via proposed method and previous studies [6, Th.14], [13], [17] when design parameter $N = 4$. As shown in this figure, the state responses reveal a better control performance by attenuating the influence of $d(t)$ compared to the previous studies.

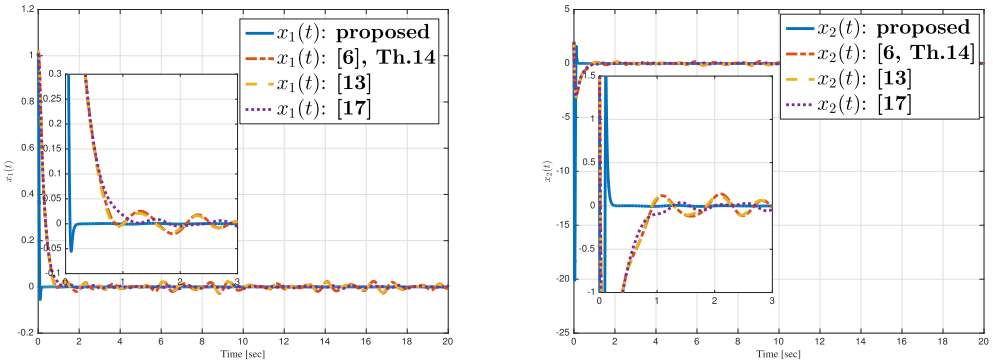

FIGURE 5. Comparison of state responses $x_1(t)$ and $x_2(t)$ via proposed method and previous studies [6, Th.14], [13], [17].

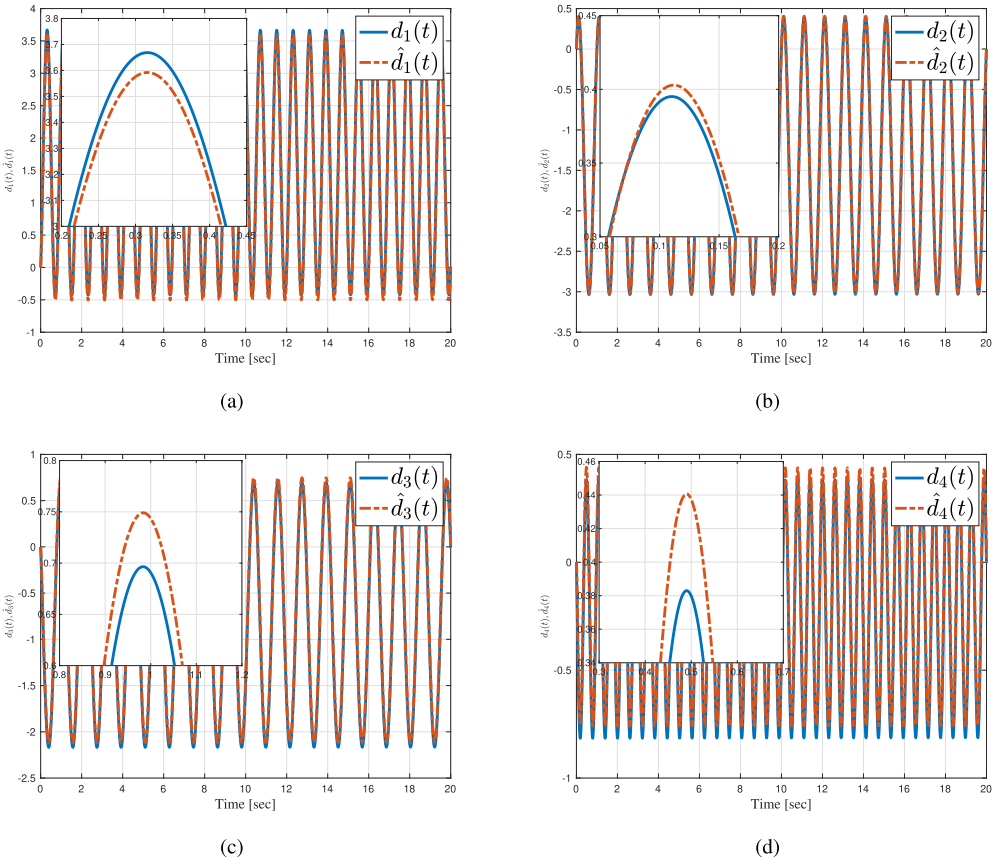

FIGURE 6. (a) - (d): Trajectories of DPS signals $d_1(t)$ to $d_4(t)$ (solid) and estimated disturbances $\hat{d}_1(t)$ to $\hat{d}_4(t)$ (dashed).

Additionally, Fig. 6 (a)-(d) show the trajectories of DPS signal $d_k(t)$ and estimated signal $\hat{d}_k(t)$ for $k \in \mathcal{I}_4$ through designed FDOBs in (15). As shown in these figures, the estimated disturbance signal $\hat{d}_k(t)$ successfully follows the DPS signal $d_k(t)$, which demonstrates that the proposed FDOBs are successfully designed. Besides, it suggests that the summation of estimation disturbances will successfully alleviate the influence of NPNS signal $d(t)$.

Furthermore, Fig. 7 (a) shows the trajectory of designed sliding surface $\mathcal{S}(t)$. As shown in this figure, the proposed sliding surface $\mathcal{S}(t)$ with the summation of estimated disturbances is successfully designed. Moreover, Fig. 7 (b) shows the energy ratio $\psi(t)$ between $y^T(t)y(t)$ and $\bar{d}^T(t)\bar{d}(t)$ in time interval $[0s\ 20s]$ under zero initial condition. As shown in this figure, the energy ratio $\psi(t)$ is less than 1.4×10^{-4}, which implies that $\sqrt{1.4\times10^{-4}} = 0.0118 < \gamma = 0.6$. Therefore, the designed controller satisfies the H_∞ control performance described in Problem 1. Finally, Fig. 7 (c) shows the trajectory of the designed controller input $u(t)$. To attenuate the influence of $d(t)$ successfully, control input $u(t)$ steadily exerts the

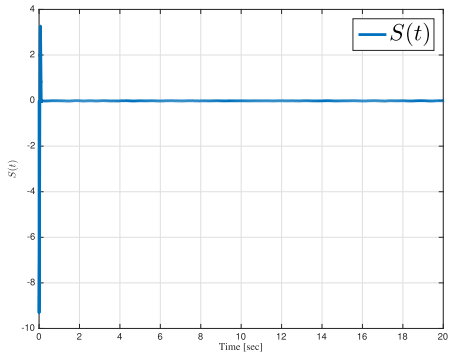

(a)

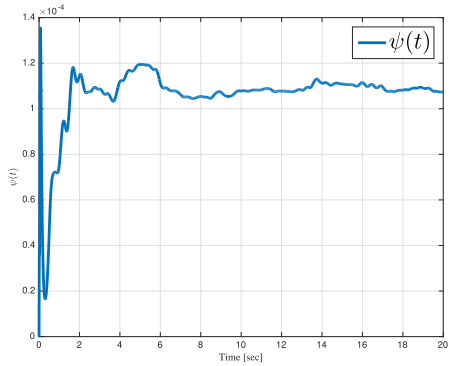

(b)

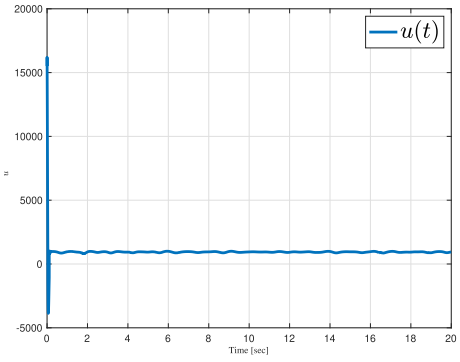

(c)

FIGURE 7. (a) Trajectory of sliding surface $\mathcal{S}(t)$; (b) trajectory of energy ratio $\psi(t)$ between $y^T(t)y(t)$ and $\bar{d}^T(t)\bar{d}(t)$ under zero initial condition; (c) trajectory of the controller input $u(t)$.

estimated disturbance $\hat{d}(t)$ derived from designed FDOBs to the T–S fuzzy model.

V. CONCLUSION AND FUTURE WORK

In this paper, a new control methodology combined with IFSMC and FDOB was proposed to enlarge design flexibility and to enhance a control performance by attenuating disturbances. The proposed method has addressed two problems: First, modification of T–S fuzzy model into a novel form enlarged design flexibility of IFSMC regardless of its fuzzy rules. Secondly, by introducing Fourier analysis, the previous DOBC concept was expanded when facing with NPNS mismatched disturbance signal generated from an exogenous system. By applying a transformed T–S fuzzy model, a novel sliding surface was suggested by summing estimated disturbances from several designed FDOBs. Besides, a sufficient condition for guaranteeing asymptotic stability of the sliding surface with H_∞ performance was proposed by using an appropriate Lyapunov function. Moreover, a reachability problem was also addressed by applying another Lyapunov function properly. Finally, the effectiveness of the proposed method was demonstrated by comparing simulation results through an inverted pendulum system.

The proposed method has demonstrated its effectiveness in dealing with the NPNS signal by designing several FDOBs via Fourier analysis, however, the developed methodology can be considered limited in that formulating FDOBs and controller with knowledge of NPNS signal. Designing FDOB and controller without knowledge of the NPNS signal is a more ideal case than the proposed method and that limitation is a still challenge to be solved. In future work, to deal with the aforementioned limitation, we will continue research by considering various NPNS signals acting on a system and then apply a regression method to identify the approximate form of NPNS signal acting on the system in advance of designing a controller and FDOBs. If we can get the approximate form of the NPNS signal, the proposed methodology will become a more suitable technique when dealing with the NPNS signal, thus, the conservativeness of the proposed method will be relaxed.

APPENDIX

A. PROOF OF THEOREM 1

Consider the following Lyapunov function candidate:

$$V(\bar{x}(t)) = \bar{x}^T(t)P\bar{x}(t), \tag{51}$$

where

$$\mathbf{0} < P = \begin{bmatrix} P_x & \mathbf{0} & \cdots & \mathbf{0} \\ \mathbf{0} & P_1 & \cdots & \mathbf{0} \\ \vdots & \vdots & \ddots & \vdots \\ \mathbf{0} & \mathbf{0} & \cdots & P_N \end{bmatrix} \in \mathcal{R}^{(n+(2N))\times(n+(2N))},$$

denotes a positive definite symmetric block matrix with $0 < P_x \in \mathcal{R}^{n\times n}$, $0 < P_1 \in \mathcal{R}^{2\times 2}$, $\cdots$, $0 < P_N \in \mathcal{R}^{2\times 2}$ and those will be determined later.

Next, a derivative of the Lyapunov candidate function (51) with respect to time can be obtained as follows:

$$\begin{aligned} \dot{V}(\bar{x}(t)) &= \dot{\bar{x}}^T(t)P\bar{x}(t) + \bar{x}^T(t)P\dot{\bar{x}}(t) \\ &= \sum_{i=1}^{r}\sum_{j=1}^{r} w_i w_j \{V_1 + V_2\}, \end{aligned} \tag{52}$$

where

$$\begin{aligned} V_1 = {} & \bar{x}^T(t)(\mathcal{A}_{ij}^T P + P\mathcal{A}_{ij})\bar{x}(t) + d^T(t)\mathcal{D}_{ij}^T P\bar{x}(t) \\ & + \bar{x}^T(t)P\mathcal{D}_{ij}d(t) + \delta^T(t)\mathcal{B}_w^T P\bar{x}(t) + \bar{x}^T(t)P\mathcal{B}_w\delta(t), \end{aligned}$$

$$V_2 = \bar{x}^T(t)(\Delta_{1j}^T P + P\Delta_{1j})\bar{x}(t) - d^T(t)\Delta_{2j}^T P\bar{x}(t) - \bar{x}^T(t)P\Delta_{2j}d(t) + \tilde{d}^T(t)\Delta_{3j}^T P\bar{x}(t) + \bar{x}^T(t)P\Delta_{3j} \times \tilde{d}(t) - E_d^T(t)\Delta_{4j}^T P\bar{x}(t) - \bar{x}^T(t)P\Delta_{4j}E_d(t).$$

To guarantee the H_∞ control performance considered in Problem 1, the following inequality should be satisfied:

$$\dot{\bar{V}}(\bar{x}(t)) = \dot{V}(\bar{x}(t)) + y^T(t)y(t) - \gamma^2\bar{d}^T(t)\bar{d}(t) < 0 = \sum_{i=1}^{r}\sum_{j=1}^{r} w_i w_j \left\{\bar{V}_1 + V_2\right\} < 0, \tag{53}$$

where

$$\bar{V}_1 = V_1 + \bar{x}^T(t)\mathcal{C}_i^T\mathcal{C}_i\bar{x}(t) - \gamma^2\left\{d^T(t)d(t) + E_d^T(t)E_d(t) + \delta^T(t)\delta(t)\right\}.$$

Therefore, if the following condition is successfully satisfied, asymptotic stability of the sliding dynamic (30) can be properly guaranteed with H_∞ control performance:

$$\bar{V}_1 + V_2 < 0. \tag{54}$$

Next, if the following condition is satisfied, the inequality (54) is also guaranteed:

$$\bar{V}_1 + V_2 < \bar{V}_1 + \bar{V}_2 < 0, \tag{55}$$

where

$$\bar{V}_2 = \bar{x}^T(t)(\Delta_{1j}^T P + P\Delta_{1j})\bar{x}(t) + d^T(t)\Delta_{2j}^T P\bar{x}(t) + \bar{x}^T(t) \times P\Delta_{2j}d(t) + \tilde{d}^T(t)\Delta_{3j}^T P\bar{x}(t) + \bar{x}^T(t)P\Delta_{3j}\tilde{d}(t) + E_d^T(t)\Delta_{4j}^T P\bar{x}(t) + \bar{x}^T(t)P\Delta_{4j}E_d(t).$$

Moreover, we can apply (7) to the first term of $\bar{V}_2$ as follows:

$$\begin{aligned}&\bar{x}^T(t)(\Delta_{1j}^T P + P\Delta_{1j})\bar{x}(t)\\ &\quad = x^T(t)K_j^T\bar{W}^T\bar{U}^T\bar{V}^T P_x x(t) + x^T(t)P_x\bar{V}\bar{U}\bar{W}K_j x(t)\\ &\quad \le x^T(t)K_j^T\bar{W}^T\bar{V}^T P_x x(t) + x^T(t)P_x\bar{V}\bar{W}K_j x(t).\end{aligned} \tag{56}$$

Next, the following inequalities also can be successfully obtained:

$$\begin{aligned}&d^T(t)\Delta_{2j}^T P\bar{x}(t) + \bar{x}^T(t)P\Delta_{2j}d(t)\\ &\quad = d^T(t)K_{dj}^T\bar{W}^T\bar{U}^T\bar{V}^T P_x x(t) + x^T(t)P_x\bar{V}\bar{U}\bar{W}K_{dj}d(t)\\ &\quad \le \alpha_1 d^T(t)K_{dj}^T\bar{W}^T\bar{W}K_{dj}d(t) + \alpha_1^{-1}x^T(t)P_x\bar{V}\bar{V}^T P_x x(t)\\ &\quad \le \alpha_1\tau_{\bar{W}}\tau_{K_d}d^T(t)d(t) + \alpha_1^{-1}\sigma_{\bar{V}}x^T(t)P_x P_x x(t),\\ &\tilde{d}^T(t)\Delta_{3j}^T P\bar{x}(t) + \bar{x}^T(t)P\Delta_{3j}\tilde{d}(t)\\ &\quad = \tilde{d}^T(t)K_{dj}^T\bar{W}^T\bar{U}^T\bar{V}^T P_x x(t) + x^T(t)P_x\bar{V}\bar{U}\bar{W}K_{dj}\tilde{d}(t)\\ &\qquad - \tilde{d}^T(t)B_{dj}^T G^T(T^{-1})^T\bar{W}^T\bar{U}^T\bar{V}^T P_x x(t) - x^T(t)P_x\bar{V}\\ &\qquad \times \bar{U}\bar{W}T^{-1}GB_{dj}\tilde{d}(t) - \tilde{d}^T(t)B_{dj}^T G^T(T^{-1})^T\bar{B}^T P_x x(t)\\ &\qquad - x^T(t)P_x\bar{B}T^{-1}GB_{dj}\tilde{d}(t)\\ &\quad \le \alpha_2\tau_{\bar{W}}\tau_{K_d}\tilde{d}^T(t)\tilde{d}(t) + \alpha_2^{-1}\sigma_{\bar{V}}x^T(t)P_x P_x x(t)\\ &\qquad + \alpha_3\tau_G\tau_{\bar{W}}\tau_{B_d}p_1^2\tilde{d}^T(t)\tilde{d}(t) + \alpha_3^{-1}\sigma_{\bar{V}}x^T(t)P_x P_x x(t)\\ &\qquad + p_1\tilde{d}^T(t)B_{dj}^T G^T\bar{B}^T P_x x(t) + p_1 x^T(t)P_x\bar{B}GB_{dj}\tilde{d}(t)\\ &\quad = \alpha_2\tau_{\bar{W}}\tau_{K_d}\bar{s}^T(t)C_{1N}^T C_{1N}\bar{s}(t) + \alpha_2^{-1}\sigma_{\bar{V}}x^T(t)P_x P_x x(t)\\ &\qquad + \alpha_3\tau_G\tau_{\bar{W}}\tau_{B_d}p_1^2\bar{s}^T(t)C_{1N}^T C_{1N}\bar{s}(t) + \alpha_3^{-1}\sigma_{\bar{V}}x^T(t)\\ &\qquad \times P_x P_x x(t) + p_1\bar{s}^T(t)C_{1N}^T B_{dj}^T G^T\bar{B}^T P_x x(t) + p_1 x^T(t)\\ &\qquad \times P_x\bar{B}GB_{dj}C_{1N}\bar{s}(t).\end{aligned} \tag{57, 58}$$

Finally, following inequality is also derived:

$$\begin{aligned}&E_d^T(t)\Delta_{4j}^T P\bar{x}(t) + \bar{x}^T(t)P\Delta_{4j}E_d(t)\\ &\quad = E_d^T(t)B_{dj}^T G^T(T^{-1})^T\bar{W}^T\bar{U}^T\bar{V}^T P_x x(t) + x^T(t)P_x\bar{V}\bar{U}\\ &\qquad \times \bar{W}T^{-1}GB_{dj}E_d(t) + E_d^T(t)B_{dj}^T G^T(T^{-1})^T\bar{B}^T P_x x(t)\\ &\qquad + x^T(t)P_x\bar{B}T^{-1}GB_{dj}E_d(t)\\ &\quad \le \alpha_4\tau_G\tau_{\bar{W}}\tau_{B_d}p_1^2E_d^T(t)E_d(t) + \alpha_4^{-1}\sigma_{\bar{V}}x^T(t)P_x P_x x(t)\\ &\qquad + p_1E_d^T(t)B_{dj}^T G^T\bar{B}^T P_x x(t) + p_1 x^T(t)P_x\bar{B}GB_{dj}E_d(t),\end{aligned} \tag{59}$$

where

$$\begin{cases}\sigma_{\bar{V}} = \lambda_{\max}(\bar{V}\bar{V}^T),\ \sigma_G = \lambda_{\max}(GG^T),\\ \sigma_{\bar{W}} = \lambda_{\max}(\bar{W}\bar{W}^T),\ \tau_{\bar{W}} = \lambda_{\max}(\bar{W}^T\bar{W}),\\ \tau_G = \lambda_{\max}(G^T G),\ \tau_{K_d} = \lambda_{\max}(K_{dj}^T K_{dj}),\\ \tau_{B_d} = \lambda_{\max}(B_{di}^T B_{di}),\\ C_{1N} = \begin{bmatrix}\bar{C}_{1d}^T & \bar{C}_{2d}^T & \cdots & \bar{C}_{Nd}^T\end{bmatrix}^T.\end{cases} \tag{60}$$

In (57) to (59), α_i with $i \in \mathcal{I}_4$ denotes proper scalar that adequately satisfies the inequality conditions. Applying these conditions, the inequality (55) can be written in block matrix form and if the following inequality is satisfied, the asymptotic stability of the sliding dynamic (31) is successfully guaranteed:

$$\bar{V}_1 + \bar{V}_2 = \bar{x}_V^T(t)\Omega_{ij}\bar{x}_V(t) < 0, \quad i, j \in \mathcal{I}_r, \tag{61}$$

where detailed descriptions of (61) are presented in (66).

Additionally, to find appropriate feedback gain matrices K_i for $i \in \mathcal{I}_r$ and FDOB gain matrices L_k for $k \in \mathcal{I}_N$, the following should be satisfied:

$$\Omega_{ij} < 0. \tag{62}$$

By applying the Schur complement to (62) and taking the congruence transformation with the following matrix:

$$\Lambda = \mathrm{diag}\left[P_x^{-1}\ I\ \cdots\ I\ I\ I\ I\right], \tag{63}$$

where Λ is a diagonal matrix with appropriate dimension, thus, we can get the following result:

$$\Theta_{ij} < 0, \tag{64}$$

where the detailed description of Θ_{ij} is also represented in (66), as shown at the bottom of the next page.

Finally, if inequalities (34) to (37) in Theorem 1 are satisfied, it implies that the asymptotic stability of the sliding dynamic (31) on the designed sliding surface $\mathcal{S}(t)$ is guaranteed, thus, the proof is completed.

Remark 8: In (60)*, the value of* τ_{B_d} *can be easily obtained because of Assumption 2. Similarly, the value of* τ_{K_d} *can be*

easily obtained since, in (20), K_{dj} *is defined as* $\bar{B}^{+}B_{dj}$, *which means that* τ_{K_d} *has the same value regardless of fuzzy rules.*

Remark 9: Moreover, the sliding dynamic (31) *is asymptotically stable if* $\Theta_{ij} < 0$ *for* $i, j \in \mathcal{I}_r$ *when* $\bar{d}(t) = 0$. *Therefore, the first condition of the Problem 1 is achieved. In addition, we can integrate* $\dot{V}(\bar{x}(t))$ *from* $t = 0$ *to* $t = \infty$ *and obtain the following result:*

$$V(\bar{x}(\infty)) - V(\bar{x}(0)) + \int_0^\infty \left(y^T(\tau)y^T(\tau) - \gamma^2 \bar{d}^T(\tau)\bar{d}(\tau) \right) d\tau < 0. \quad (65)$$

Next, by using a condition $V(\bar{x}(\infty)) \geq 0$, (65) *implies the following:*

$$\int_0^\infty \left(y^T(\tau)y^T(\tau) - \gamma^2 \bar{d}^T(\tau)\bar{d}(\tau) \right) d\tau < V(\tilde{x}(0)) - V(\tilde{x}(\infty)) \leq \tilde{x}^T(0)P\tilde{x}(0).$$

Therefore, under initial condition $\bar{x}^T(0)P\bar{x}(0) = 0$, *the energy ratio between* $y^T(t)y(t)$ *and* $\bar{d}^T(t)\bar{d}(t)$, $\psi(t) < 0$ *is achieved. Finally, the second condition of the Problem 1 also holds.*

B. DETAILED ILLUSTRATION OF SECTION II.B

In this subsection, a detailed procedure of filtering out distinct DPS signals of NPNS signal $d(t)$ via Fourier analysis by using a form of (11) is provided.

Before proceeding, the following formula is a Fourier transform which has used for a long time in many engineering fields [27]:

$$X(f) = \int_{-\infty}^{\infty} x(t)e^{-i2\pi ft}dt, \quad (67)$$

$$x(t) = \int_{-\infty}^{\infty} X(f)e^{i2\pi ft}df, \quad (68)$$

where $x(t)$ is an integrable function satisfying $x : \mathcal{R} \to \mathcal{C}$, and $X(f)$ is a Fourier coefficient, which is a complex number having information about the magnitude and phase at a certain frequency.

Moreover, by Euler formula, complex value $X(f)$ can be represented as follows:

$$X(f) = X_R + iX_I = |X_A|\, e^{i\theta}, \quad (69)$$

where $|X_A| = \sqrt{X_R^2 + X_I^2}$, and $\theta = \tan^{-1}\left(\frac{X_I}{X_R}\right)$. Next, substituting (69) into (68), the following result can be obtained:

$$x(t) = \int_{-\infty}^{\infty} |X_A|\, e^{i(2\pi ft+\theta)}df = \int_{-\infty}^{\infty} |X_A| \left(\cos(2\pi ft + \theta) + i\sin(2\pi ft + \theta)\right) df.$$

$$\Omega_{ij} = \begin{bmatrix} He\{A_i^T P_x + K_j^T \bar{B}^T P_x\} + \Pi_\Omega & * & * & * & * & * & * \\ \bar{C}_{1d}^T \left(\Gamma_j^T + p_1\, B_{di}^T G^T \bar{B}^T\right) P_x & \mu_1 & * & * & * & * & * \\ \vdots & \vdots & \ddots & * & * & * & * \\ \bar{C}_{Nd}^T \left(\Gamma_j^T + p_1\, B_{di}^T G^T \bar{B}^T\right) P_x & \mathbf{0} & \mathbf{0} & \mu_N & * & * & * \\ B_{di}^T - K_{dj}^T \bar{B}^T P_x & \mathbf{0} & \mathbf{0} & \mathbf{0} & (h_1 - \gamma^2)I & * & * \\ \mathbf{0} & B_{w1}^T P_1 & \cdots & B_{wN}^T P_N & \mathbf{0} & -\gamma^2 I & * \\ p_1\, B_{di}^T G^T \bar{B}^T P_x & \mathbf{0} & \mathbf{0} & \mathbf{0} & \mathbf{0} & \mathbf{0} & (h_2 - \gamma^2)I \end{bmatrix},$$

$$\Pi_\Omega = He\left\{P_x \bar{V} \bar{W} K_j\right\} + (\alpha_1^{-1} + \alpha_2^{-1} + \alpha_3^{-1} + \alpha_4^{-1})\sigma_{\bar{V}} P_x P_x + C_i^T C_i,$$

$$\mu_1 = He\{\bar{A}_{1d}^T P_1 - \bar{C}_{1d}^T B_{di}^T Y_1^T\} + \alpha_2 \tau_{\bar{W}} \tau_{K_d} \bar{C}_{1d}^T \bar{C}_{1d} + \alpha_3 \tau_G \tau_{\bar{W}} \tau_{B_d} p_1^2 \bar{C}_{1d}^T \bar{C}_{1d},$$

$$\mu_N = He\{\bar{A}_{Nd}^T P_N - \bar{C}_{Nd}^T B_{di}^T Y_N^T\} + \alpha_2 \tau_{\bar{W}} \tau_{K_d} \bar{C}_{Nd}^T \bar{C}_{Nd} + \alpha_3 \tau_G \tau_{\bar{W}} \tau_{B_d} p_1^2 \bar{C}_{Nd}^T \bar{C}_{Nd},$$

$$h_1 = \alpha_1 \tau_{\bar{W}} \tau_{Kd},\ h_2 = \alpha_4 \tau_G \tau_{\bar{W}} \tau_{B_d} p_1^2,$$

$$\Theta_{ij} = \begin{bmatrix} He\{XA_i^T + N_j^T \bar{B}^T\} + \Pi_\Theta & * & * & * & * & * & * & * \\ \bar{C}_{1d}^T \left(\Gamma_j^T + p_1\, B_{di}^T G^T \bar{B}^T\right) & \mu_1 & * & * & * & * & * & * \\ \vdots & \vdots & \ddots & * & * & * & * & * \\ \bar{C}_{Nd}^T \left(\Gamma_j^T + p_1\, B_{di}^T G^T \bar{B}^T\right) & \mathbf{0} & \mathbf{0} & \mu_N & * & * & * & * \\ B_{di}^T - K_{dj}^T \bar{B}^T & \mathbf{0} & \mathbf{0} & \mathbf{0} & (h_1 - \gamma^2)I & * & * & * \\ \mathbf{0} & B_{w1}^T P_1 & \cdots & B_{wN}^T P_N & \mathbf{0} & -\gamma^2 I & * & * \\ p_1 B_{di}^T G^T \bar{B}^T & \mathbf{0} & \mathbf{0} & \mathbf{0} & \mathbf{0} & \mathbf{0} & (h_2 - \gamma^2)I & * \\ C_i X & \mathbf{0} & \mathbf{0} & \mathbf{0} & \mathbf{0} & \mathbf{0} & \mathbf{0} & -I \end{bmatrix},$$

$$\Pi_\Theta = He\left\{P_x \bar{V} \bar{W} N_j\right\} + (\alpha_1^{-1} + \alpha_2^{-1} + \alpha_3^{-1} + \alpha_4^{-1})\sigma_{\bar{V}},$$

$$\bar{x}_V(t) = \begin{bmatrix} x^T(t) & \bar{s}^T(t) & d^T(t) & \delta^T(t) & E_d^T(t) \end{bmatrix}^T,$$

where $X = P_x^{-1}, N_j = K_j X^{-1}, L_i = P_i^{-1} Y_i$, for $j \in \mathcal{I}_r$ and $i \in \mathcal{I}_N$. (66)

If we consider $x(t)$ as a real-valued function, $x(t)$ can be regarded as follows:

$$x(t) = \int_{-\infty}^{\infty} |X_A| \cos(2\pi ft + \theta) df. \tag{70}$$

Remark 10: The result of (70) *implies that if we can find out Fourier coefficient $X(f)$ at a certain frequency (i.e. the magnitude and phase information of that frequency are obtained), $x(t)$ can be represented as a linear summation of sinusoid signals.*

If we regard $x(t)$ as $d(t)$, representing $d(t)$ with several DPS signals can be possible by virtue of Fourier analysis. Next, consider the following first-order linear differential equation form as described in (11):

$$\begin{cases} \dot{q}(t) = \begin{bmatrix} 0 & \lambda \\ -\lambda & 0 \end{bmatrix} q(t) + \begin{bmatrix} b_{w1} \\ b_{w2} \end{bmatrix} \delta(t), \\ s(t) = \begin{bmatrix} c_1 & c_2 \end{bmatrix} q(t), \end{cases} \tag{71}$$

where $q(t) \in \mathcal{R}^2$ is a state of differential equation satisfying $q(t) = \left[q_1^T(t)\ q_2^T(t)\right]^T$, $s(t) \in \mathcal{R}^1$ is a output, $\lambda \in \mathcal{R}^1$, $b_{w1} \in \mathcal{R}^1$, $b_{w2} \in \mathcal{R}^1$, $c_1 \in \mathcal{R}^1$, and $c_2 \in \mathcal{R}^1$ are constant values to be determined, and $\delta(t)$ is a constant signal with a value of 1. If we assume the initial value of $q(0) = 0$, the general solution of $q(t)$ can be obtained as follows:

$$\begin{cases} q_1(t) = \dfrac{b_{w2}}{\lambda} - \dfrac{b_{w2}}{\lambda}\cos(\lambda t) + \dfrac{b_{w1}}{\lambda}\sin(\lambda t), \\ q_2(t) = -\dfrac{b_{w1}}{\lambda} + \dfrac{b_{w2}}{\lambda}\sin(\lambda t) + \dfrac{b_{w1}}{\lambda}\cos(\lambda t). \end{cases} \tag{72}$$

Moreover, applying sinusoid summation formulas, (72) can be written as follows:

$$\begin{cases} q_1(t) = \dfrac{b_{w2}}{\lambda} + \dfrac{\sqrt{b_{w1}^2 + b_{w2}^2}}{\lambda} \cos\left(\lambda t - \theta_1\right), \\ q_2(t) = -\dfrac{b_{w1}}{\lambda} + \dfrac{\sqrt{b_{w1}^2 + b_{w2}^2}}{\lambda} \cos\left(\lambda t - \theta_2\right), \\ s(t) = c_1 q_1(t) + c_2 q_2(t), \end{cases}$$

where $\theta_1 = \tan^{-1}\left(\frac{b_{w1}}{-b_{w2}}\right)$, $\theta_2 = \tan^{-1}\left(\frac{b_{w2}}{b_{w1}}\right)$.

To reduce computation and concise interpretation, we can choose $c_2 = 0$, which means that the output of differential equation (71) only depends on $q_1(t)$. Thus, the following result can be obtained:

$$s(t) = \frac{c_1\sqrt{b_{w1}^2 + b_{w2}^2}}{\lambda}\cos\left(\lambda t - \theta_1\right) + \frac{c_1 b_{w2}}{\lambda}.$$

Therefore, if we appropriately choose constant values λ, b_{w1}, b_{w2}, and c_1 by considering the magnitude and phase information of $X(f)$ at the specific frequency, it is possible to generate a periodic sinusoid signal with specific characteristics, such as frequency, phase, and magnitude via the form of (71). Likewise, using the above procedure, we can also generate other periodic sinusoid signals which largely account for the original signal $d(t)$ via the structure of (71).

To sum up, if we combine output signals derived from several differential equation forms with (71), it is possible to approximately obtain the original NPNS signal $d(t)$ as (12).

REFERENCES

[1] C. T. Chen, *Linear System Theory and Design*, 3rd ed. New York, NY, USA: Oxford Univ. Press, 2009.
[2] D. G. Luenberger, *Introduction to Dynamic Systems Theory, Models, and Applications*. New York, NY, USA: Wiley, 1979.
[3] J. J. E. Slotine and W. Li, *Applied Nonlinear Control*. Englewood Cliffs, NJ, USA: Prentice-Hall, 1991.
[4] H. K. Khalil, *Nonlinear System*, 3rd ed. London, U.K.: Pearson, 2001.
[5] T. Takagi and M. Sugeno, "Fuzzy identificaion of systems and its application to modeling and control," *IEEE Trans. Syst., Man, Cybern., Syst.*, vol. SMC-15, no. 1, pp. 116–132, Jan. 1985.
[6] K. Tanaka and H. Wang, *Fuzzy Control Systems Design and Analysis: A Linear Matrix Inequality Approach*. New York, NY, USA: Wiley, 2002.
[7] H. J. Kim, J. B. Park, and Y. H. Joo, "H_∞ fuzzy filter for non-linear sampled-data systems under imperfect premise matching," *IET Control Theory Appl.*, vol. 11, no. 5, pp. 747–755, Mar. 2017.
[8] H. J. Kim, J. B. Park, and Y. H. Joo, "Intelligent digital redesign for T–S fuzzy systems: Sampled-data filter approach," *IET Control Theory Appl.*, vol. 12, no. 9, pp. 1306–1317, Jun. 2018.
[9] C.-S. Tseng, B.-S. Chen, and H.-J. Uang, "Fuzzy tracking control design for nonlinear dynamic systems via T-S fuzzy model," *IEEE Trans. Fuzzy Syst.*, vol. 9, no. 3, pp. 381–392, Jun. 2001.
[10] H. J. Kim, J. B. Park, and Y. H. Joo, "Sampled-data H_∞ fuzzy observer for uncertain oscillating systems with immeasurable premise variables," *IEEE Access*, vol. 6, pp. 58075–58085, 2018.
[11] H. S. Kim, J. B. Park, and Y. H. Joo, "Decentralized sampled-data tracking control of large-scale fuzzy systems: An exact discretization approach," *IEEE Access*, vol. 5, pp. 12668–12681, 2017.
[12] H. Jae Lee, J. Bae Park, and G. Chen, "Robust fuzzy control of nonlinear systems with parametric uncertainties," *IEEE Trans. Fuzzy Syst.*, vol. 9, no. 2, pp. 369–379, Apr. 2001.
[13] H. Li, J. Yu, C. Hilton, and H. Liu, "Adaptive sliding-mode control for nonlinear active suspension vehicle systems using T–S fuzzy approach," *IEEE Trans. Ind. Electron.*, vol. 60, no. 8, pp. 3328–3338, Aug. 2013.
[14] Y. Wang, H. Shen, H. R. Karimi, and D. Duan, "Dissipativity-based fuzzy integral sliding mode control of continuous-time T–S fuzzy systems," *IEEE Trans. Fuzzy Syst.*, vol. 26, no. 3, pp. 1164–1176, Jun. 2018.
[15] Z. Xi, G. Feng, and T. Hesketh, "Piecewise integral sliding-mode control for T–S fuzzy systems," *IEEE Trans. Fuzzy Syst.*, vol. 19, no. 1, pp. 65–74, Feb. 2011.
[16] S. Hwang, J. B. Park, and Y. H. Joo, "Disturbance observer-based integral fuzzy sliding-mode control and its application to wind turbine system," *IET Control Theory Appl.*, vol. 13, no. 12, pp. 1891–1900, Aug. 2019.
[17] H.-N. Wu, Z.-Y. Liu, and L. Guo, "Robust L_∞-gain fuzzy disturbance observer-based control design with adaptive bounding for a hypersonic vehicle," *IEEE Trans. Fuzzy Syst.*, vol. 22, no. 6, pp. 1401–1412, Dec. 2014.
[18] V. Utkin and J. Shi, "Integral sliding mode in systems operating under uncertainty conditions," in *Proc. 35th IEEE Conf. Decis. Control*, Kobe, Japan, Dec. 1996, pp. 4591–4596.
[19] K. Ohishi, M. Nakao, K. Ohnishi, and K. Miyachi, "Microprocessor-controlled DC motor for load-insensitive position servo system," *IEEE Trans. Ind. Electron.*, vol. IE-34, no. 1, pp. 44–49, Feb. 1987.
[20] W.-H. Chen, "Disturbance observer based control for nonlinear systems," *IEEE/ASME Trans. Mechatronics*, vol. 9, no. 4, pp. 706–710, Dec. 2004.
[21] S. Li, J. Yang, W. H. Chen, and X. Chen, *Disturbance Observer-Based Control Methods and Applications*, 1st ed. Boca Raton, FL, USA: CRC Press, 2014.
[22] M. Chen and W.-H. Chen, "Disturbance-observer-based robust control for time delay uncertain systems," *Int. J. Control, Autom. Syst.*, vol. 8, no. 2, pp. 445–453, Apr. 2010.
[23] J. Zhang, X. Liu, Y. Xia, Z. Zuo, and Y. Wang, "Disturbance observer-based integral sliding-mode control for systems with mismatched disturbances," *IEEE Trans. Ind. Electron.*, vol. 63, no. 11, pp. 7040–7048, Nov. 2016.
[24] H. H. Choi, "Robust stabilization of uncertain fuzzy systems using variable structure system approach," *IEEE Trans. Fuzzy Syst.*, vol. 16, no. 3, pp. 715–724, Jun. 2008.

[25] C. Han, G. Zhang, L. Wu, and Q. Zeng, "Sliding mode control of T–S fuzzy descriptor systems with time-delay," *J Franklin I.*, vol. 349, no. 4, pp. 1430–1444, May 2012.
[26] J. Li, Q. Zhang, X.-G. Yan, and S. K. Spurgeon, "Observer-based fuzzy integral sliding mode control for nonlinear descriptor systems," *IEEE Trans. Fuzzy Syst.*, vol. 26, no. 5, pp. 2818–2832, Oct. 2018.
[27] S. Brunton and J. N. Kutz, *Data-Driven Science and Engineering: Machine Learning, Dynamical Systems, and Control*, 1st ed. Cambridge, U.K.: Cambridge Univ. Press, 2019.
[28] H. K. Lam and L. D. Seneviratne, "Stability analysis of interval type-2 fuzzy-model-based control systems," *IEEE Trans. Syst., Man, Cybern. B, Cybern.*, vol. 38, no. 3, pp. 617–628, Jun. 2008.
[29] S. H. Hwang, J. B. Park, and Y. H. Joo, "Disturbance observer-based H_∞ control of the T–S fuzzy model under imperfect premise matching," in *Proc. IEEE/ASME Int. Conf. Adv. Intell. Mechatronics*, Aukland, New Zealand, Jul. 2018, pp. 622–627.
[30] W. H. Chen, J. Yang, L. Guo, and S. Li, "Disturbance-observer-based control and related methods—An overview," *IEEE Trans. Ind. Electron.*, vol. 63, no. 2, pp. 1083–1095, Feb. 2016.
[31] G. Strang, *Introduction to Linear Algebra*, 5th ed. Cambridge, MA, USA: Wellesley-Cambridge, 2016.
[32] D. Ginoya, P. D. Shendge, and S. B. Phadke, "Sliding mode control for mismatched uncertain systems using an extended disturbance observer," *IEEE Trans. Ind. Electron.*, vol. 61, no. 4, pp. 1983–1992, Apr. 2014.
[33] J. Yang, S. Li, and X. Yu, "Sliding-mode control for systems with mismatched uncertainties via a disturbance observer," *IEEE Trans. Ind. Electron.*, vol. 60, no. 1, pp. 160–169, Jan. 2013.
[34] J. Li, Q. Zhang, X.-G. Yan, and S. K. Spurgeon, "Robust stabilization of T–S fuzzy stochastic descriptor systems via integral sliding modes," *IEEE Trans. Cybern.*, vol. 48, no. 9, pp. 2736–2749, Sep. 2018.
[35] K. Mei and S. Ding, "Second-order sliding mode controller design subject to an upper-triangular structure," *IEEE Trans. Syst., Man, Cybern., Syst.*, early access, Nov. 5, 2019, doi: 10.1109/TSMC.2018.2875267.
[36] S. Ding, J. H. Park, and C.-C. Chen, "Second-order sliding mode controller design with output constraint," *Automatica*, vol. 112, Feb. 2020, Art. no. 108704.
[37] G. Bartolini, A. Pisano, E. Punta, and E. Usai, "A survey of applications of second-order sliding mode control to mechanical systems," *Int. J. Control*, vol. 76, nos. 9–10, pp. 875–892, Jan. 2003.
[38] G. Bartolini, A. Ferrara, and E. Usai, "Chattering avoidance by second-order sliding mode control," *IEEE Trans. Autom. Control*, vol. 43, no. 2, pp. 241–246, Feb. 1998.
[39] X.-H. Chang and G.-H. Yang, "Nonfragile H_∞ filtering of continuous-time fuzzy systems," *IEEE Trans. Signal Process.*, vol. 59, no. 4, pp. 1528–1538, Apr. 2011.
[40] X.-H. Chang, J. Xiong, and J. H. Park, "Estimation for a class of parameter-controlled tunnel diode circuits," *IEEE Trans. Syst., Man, Cybern., Syst.*, early access, Aug. 13, 2018, doi: 10.1109/TSMC.2018.2859933.
[41] Z.-M. Li, X.-H. Chang, and J. H. Park, "Quantized static output feedback fuzzy tracking control for discrete-time nonlinear networked systems with asynchronous event-triggered constraints," *IEEE Trans. Syst., Man, Cybern., Syst.*, early access, Aug. 15, 2019, doi: 10.1109/TSMC.2019.2931530.
[42] S. Ding and S. Li, "Second-order sliding mode controller design subject to mismatched term," *Automatica*, vol. 77, pp. 388–392, Mar. 2017.
[43] C. Garcia, D. Prett, and M. Morari, "Model predictive control: Theory and practice—A survey," *Automatica*, vol. 25, no. 3, pp. 335–348, Oct. 1988.
[44] F.-J. Lin, Y.-C. Hung, and K.-C. Ruan, "An intelligent second-order sliding-mode control for an electric power steering system using a wavelet fuzzy neural network," *IEEE Trans. Fuzzy Syst.*, vol. 22, no. 6, pp. 1598–1611, Dec. 2014.

SOUNGHWAN HWANG received the B.S. degree from the Division of Robotics, Kwangwoon University, in 2017, and the M.S. degree in electrical and electronic engineering from Yonsei University, Seoul, South Korea, in 2019. His current research interests include control theory, fuzzy control, nonlinear system analysis, and model predictive control.

HAN SOL KIM received the B.S. degree in electronic and computer engineering from Hanyang University, South Korea, in 2011, and the M.S. and Ph.D. degrees in electrical and electronic engineering from Yonsei University, South Korea, in 2012 and 2018, respectively. He worked as a Senior Engineer with Samsung Electronics Company, South Korea, from 2018 to 2019. Since 2019, he has been with the Department of Control and Automation Engineering, National Korea Maritime and Ocean University, where he is currently an Assistant Professor. His current research interests include intelligent robot, intelligent control, and unmanned aerial vehicles.